# Eu(iii) and Tb(iii) complexes of 6-fold coordinating ligands showing high affinity for the hydrogen carbonate ion: A spectroscopic and thermodynamic

# Eu(III) and Tb(III) complexes of 6-fold coordinating ligands showing high affinity for the hydrogen carbonate ion: a spectroscopic and thermodynamic study

Fabio Piccinelli,*[1] Chiara De Rosa,[1] Andrea Melchior,*[2] Georgina Faura,[2] Marilena Tolazzi,[2] and Marco Bettinelli[1]

[1] Laboratorio Materiali Luminescenti, DB, Università di Verona, and INSTM, UdR Verona, Strada Le Grazie 15, 37134 Verona, Italy

[2] Dipartimento Politecnico di Ingegneria e Architettura, Laboratorio di Tecnologie Chimiche, Università di Udine, via Cotonificio 108, 33100 Udine, Italy

**Keywords**

Eu(III) and Tb(III), luminescence, ligand synthesis, stability constants, DFT calculations, hydrogen carbonate sensing.

**Abstract**

In the present contribution, four classes of Ln(III) complexes (Ln = Eu and Tb) have been synthesized and characterized in aqueous solution. They differ by charge, **Ln(bpcd)**$^{+}$ [bpcd$^{2-}$ = N,N′-bis(2-pyridylmethyl)-trans-1,2-diaminocyclohexane N,N′-diacetate] and **Ln(bQcd)**$^{+}$ (bQcd$^{2-}$ = N,N′-bis(2-quinolinmethyl)-trans-1,2-diaminocyclohexane N,N′-diacetate) being positively charged and **Ln(PyC3A)** (**PyC3A**$^{3-}$ = N-picolyl-N,N',N'-trans-l,2-cyclohexylenediaminetriacetate) and **Ln(QC3A)** (**QC3A**$^{3-}$ **=** N-quinolyl-N,N',N'-trans-l,2-cyclohexylenediaminetriacetate) neutral. Combined DFT, spectrophotometric and potentiometric studies reveal the presence, in physiologic condition (pH 7.4), of a couple of equally and highly stable isomers differing by the stereochemistry of the ligands (*trans*-N,N and *trans*-O,O for bpcd$^{2-}$ and bQcd$^{2-}$; *trans*-O,O and *trans*-N,O for PyC3A$^{3-}$ and QC3A$^{3-}$). Their high log$\beta$ values (9.97 <log$\beta$< 15.68), the presence of an efficient *antenna effect* and the strong increase of the Ln(III) luminescence intensity as a function of the hydrogen carbonate concentration in physiologic solution, candidate these complexes as very promising optical probes for a selective detection of $HCO_3^-$ *in cellulo* experiments or in extracellular fluid. This particularly applies to the cationic **Eu(bpcd)**$^{+}$, **Tb(bpcd)**$^{+}$ and **Eu(bQcd)**$^{+}$ complexes, which are capable to guest

up to two hydrogen carbonate anions in the inner coordination sphere of the metal ion, so that they show an unprecedented affinity towards $HCO_3^-$ (log*K* for the formation of the adduct in the 4.6-5.9 range).

## Introduction

Eu(III) and Tb(III) complexes have been broadly exploited as efficient optical probes in the field of bioimaging and sensing[1–6] due to the peculiar properties of their $f \leftrightarrow f$ transitions, such as long luminescence lifetime and large energy difference between the absorbing and emissive states. These advantageous properties allow to mitigate the interference of background fluorescence originating from the biological sample and to remove self-absorption issues, respectively. Thanks to both the lack of self-absorption and the usual low concentration of the optical probe, which ensures absorbance below 0.1 at the excitation wavelength, the intensity of the luminescence signal of the complexes is proportional to their concentration over a wide range of values. With this in mind, lanthanide-based molecular probes have been employed for the detection of the pH[7] and intracellular analytes such as ATP.[8] The optical properties of the complexes are strongly dependent on the nature of the ligand; the luminescence stemming from the metal ion can be conveniently sensitized if the ligand is capable to strongly absorb and efficiently transfer the UV excitation to the metal ion (*antenna* effect). Furthermore, solvent molecules usually give rise to competitive non-radiative mechanisms such as the multiphonon relaxation process. On the basis of the "energy gap law", if the gap between the emitting level and the one below is bridged by less than four vibrational quanta, the multiphonon relaxation process significantly works and the luminescence quantum yield will be low.[9,10] The high energy of the O-H vibrations in the water molecules is particularly efficient in the non-radiative quenching of the emitting level and this phenomenon is especially relevant for applications in biomedicine, where aqueous media are commonly employed. Nevertheless, Eu(III) and mainly Tb(III) are less affected by the multiphonon relaxation process as the energy gap between the emitting level and the lower lying ones is relatively large [about 12400 $cm^{-1}$ for Eu(III) and 14800 $cm^{-1}$ for Tb(III)].[11]

As far as optical sensing experiments based on luminescent lanthanide complexes are concerned, the displacement of water molecules from the inner coordination sphere of the metal ion by the target molecule is often employed. This displacement gives rise to an increase of the quantum yield and the concomitant increase of the luminescent intensity could be linked to the concentration of the analyte in solution.

Another important factor that must not be neglected when the compounds are used in *in vitro* experiments is the impact of the hydrophobicity and charge of lanthanide metal complexes on the cell viability and cell association,[12] including their membrane permeability.[13–17] The *in vitro* localization of the optical probe affects the type of analytes that can be detected. For example, a probe with an extracellular location is particularly suitable to detect analytes such as group I ions, polysaccharides, hormones, or other signaling molecules.[12]

Another crucial aspect to consider is the selectivity of the optical response towards a particular analyte. In this context, the modulation of the structure of the side pendants within the DO3A-based complexes gave the best results when serum proteins and biological relevant ions are taken into account.[18–21]

In summary, charge and lipophilicity of the probe and selectivity towards a particular target analyte are crucial properties that must be considered when designing a complex with potential application in optical sensing of biological relevant species. In line with a natural extension of a recent structural and spectroscopic study, performed by some of us, on a promising chiro-optical probe based on a Tb(III) complex of a polyaminocarboxylate ligand [N,N′-bis(2-pyridylmethyl)-trans-1,2-diaminocyclohexaneN,N′-diacetic acid ($H_2$bpcd)][18,19], we propose a new library of ligands and its relative Eu(III) and Tb(III) complexes, based on the chiral diaminocyclohexane (DACH) motif (Figure 1).[22–25]

The proposed water-soluble complexes differ: i) by charge, since Ln(bpcd)$^+$ and Ln(bQcd)$^+$ are cationic whilst Ln(PyC3A) and Ln(QC3A) are neutral, ii) by steric hindrance at the metal ion, which is big in the case of Ln(bQcd)$^+$ and small in the case of Ln(PyC3A) and iii) by lipophilicity, the molecules containing the quinoline fragment being more hydrophobic than the relative pyridine-based ones. Total charge and steric hindrance are expected to have a strong impact on the stability of both the complexes and their adducts with target analytes so as to enable the opportunity of a selective probe-target interaction. In addition, in the light of the lower number of donating atoms (6-fold coordination) for ligands in figure 1 than in the case of ligands commonly employed for Ln(III)-based luminescence anion sensing (NOTA and DOTA-like possessing 7-fold coordination), we expect a higher number of target analyte molecules bound to the metal ion and a concomitant higher affinity towards them. This should be particularly true when non-sterically demanding anion are considered. Apart from monoatomic anions, also hydrogen carbonate ($HCO_3^-$) meets this requirement and, in addition, it plays a crucial role in many physiologic processes[26] including intracellular pH homeostasis, kidney function and sperm maturation, and therefore must be considered an important target in probe development. Moreover, the $HCO_3^-$ concentration is critical in assessing metabolic

acidosis, that is abnormally increased hydrogen ion concentration. Patients with chronic kidney disease due to metabolic acidosis show low serum hydrogen carbonate concentrations.[27,28] For all these reasons, in the present contribution we present the synthesis, the optical spectroscopy, the thermodynamic and structural characterization in aqueous solution of the Eu(III) and Tb(III) complexes presented in figure 1. The good performance of these molecules for the optical detection of hydrogen carbonate anion in physiological conditions is also documented and analyzed in relation to the aforementioned properties of the complexes (i.e. total charge, steric hindrance, etc.)

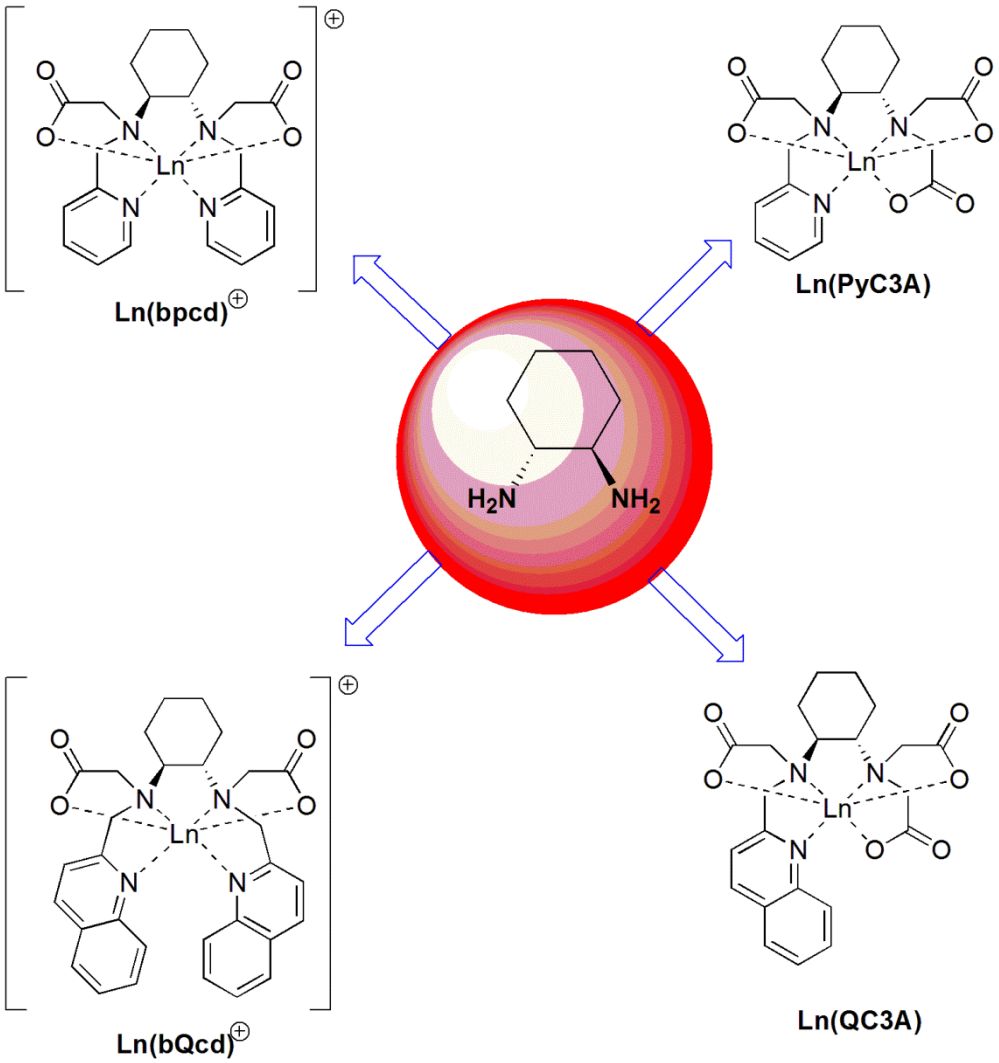


**Figure 1.** Library of the complexes presented in this contribution: $Ln(bQcd)^+$ and $Ln(bpcd)^+$ are cationic complexes; Ln(QC3A) and Ln(PyC3A) are neutral complexes. The solvent molecules bound to the metal ion are omitted for the sake of clarity.

**Experimental Section**

All commercially available reagents were used as received from their respective suppliers. Solvents, (Sigma-Aldrich) were dried when required using an appropriate drying agent. Reactions requiring anhydrous conditions were carried out using Schlenk-line techniques under an atmosphere of dry argon. Water and $H_2O$ refer to high purity water obtained from the 'Millipore Elix 10' purification system. $Eu(CF_3SO_3)_3$ and $TbCl_3 \cdot 6H_2O$ (Aldrich, 98%) were stored under vacuum for several days at 80°C and then transferred to the glove box. All other chemicals were purchased from Alfa Aesar.
Thin-layer chromatography was carried out on neutral alumina plates (Fluka Analytical) or silica plates (Sigma-Aldrich) and visualized under UV lamp (254 nm). The cationic exchange chromatography was performed on SCX cartridges (1g) purchased from "Agilent Technologies-sample Prep solutions".

*N,N'-bis(2-quinolinmethyl)-trans-1,2-diaminocyclohexane N,N'- tert-butyl diacetate (1R, 2R)***(2)**: Ligand **1** (1.8 g, 4.54 mmol) was dissolved in a mixture of anhydrous acetonitrile (80 mL) and anhydrous potassium carbonate under inert condition (Argon). Then, a solution of tert-Butyl 2-bromoacetate (1.68 ml, 11.4 mmol), in anhydrous acetonitrile (15 mL) was added dropwise over ten minutes. After stirring 12 h at room temperature dichloromethane was added and the reaction mixture was washed with brine solution. The organic phase was evaporated under reduced pressure to give 3.3 g of a yellowish oil. The crude product was purified by chromatography on activated neutral alumina ($Al_2O_3$, Cy:AcOEt from 9:1 to 1:9) giving 2.50 g of a yellowish oil (yield: 88%). $^1$H-NMR ($CDCl_3$) δ (ppm) 8.07-8.04 (m, 4H, quinoline), 7.92 (d, J=7.76 Hz, 2H, quinoline), 7.75 (d, J= 7.10 Hz, 2H, quinoline), 7.69 (7, J=7.68 Hz, 2H, quinoline), 7.50 (t, J=7.40 Hz, 2H, quinoline), 4.16 (m, 2H, methylene-ester), 3.86 (d, $J_{GEM}$=13.75 Hz, 2H, methylene-ester), 3.49 (d, $J_{GEM}$=17.22 Hz, 2H, methylene-quinoline), 3.31 (d, $J_{GEM}$=17.22 Hz, 2H, methylene-quinoline), 2.71 (m, 2H, methylene-cyclohexane), 2.18-1.12 (m, 8H, cyclohexane), 1.46 (s, 18H). $^{13}$C-NMR ($CDCl_3$) δ (ppm) 173.0, 159.3, 148.5, 135.3, 129.4, 129.0, 127.1, 125.8, 125.0, 122.0, 73.5, 57.8, 55.1, 53.7, 29.2, 26.7, 22.0. Elemental Anal. Calc. for $C_{38}H_{48}N_4O_4$ (MW 624,8): C, 73.05; H, 7.74; N, 8.97; O, 10.24 Found: C, 72.89 ; H, 7.51; N, 9.03; O, 10.36

*N,N'-bis(2-quinolinmethyl)-trans-1,2-diaminocyclohexane N,N'-diacetic acid (1R, 2R)* (**$H_2$bQcd**, ligand **3** as ammonium salt): **2** (1.20 g, 1.92 mmol) was dissolved in HCl aq (6 M, 30 ml); the obtained reaction mixture was stirred for 12 h at 80°C. The reaction mixture was washed with ethyl acetate and the aqueous phase was evaporated under reduced pressure. The obtained brownish oil (2.47 g)

was suspended in 10 ml of methanol, aqueous ammonia solution was added until pH 8-9 was reached and 1.05 g of a yellowish solid were obtained after chromatography [(C18 column; eluent $H_2O$:Acetonitrile 4:6 +0.1% $NH_4OH$ aq 30% w/w (50 ml)]. This solid was further purified by trituration in DCM:AcOEt:EtOH 1:2:2 at 80 °C for 30 minutes, obtaining 548 mg of a yellowish solid (ligand **3**, yield: 52%). UV-Vis absorption spectroscopy (water:methanol 9:1): ε(316 nm): 6728 $M^{-1}cm^{-1}$. $^1$H-NMR ($CD_3OD$) δ (ppm) 8.05-7.48 (m, 12H, quinoline), 3.74-3.55 (m, 8H, methylene-ester/quinoline), 2.39 (m, 2H, cyclohexane), 1.98 (m, 2H, cyclohexane), 1.67-1.28 (m, 6H, cyclohexane). INSERIE C13. UV-Vis spectroscopy: ε(316 nm)= 6248 $M^{-1}cm^{-1}$ (methanol). Elemental Anal. Calc. for $C_{30}H_{38}N_6O_4$ (MW 546.7): C, 65.91; H, 7.01; N, 15.37; O, 11.71 Found: C, 65.79 ; H, 7.09; N, 15.27; O, 11.59

The triflate of the cationic complex Eu(bQcd) (complex **4**) has been synthesized as follows: Ligand **3** (100 mg, 0.182 mmol) was dissolved in hot (60°C) 2-propanol (7 ml). Upon cooling, europium(III) trifluoromethanesulfonate 98% (109 mg, 0.182 mmol) was added portion-wise, and a yellowish suspension was formed. After neutralization with KOH 2M aq (pH ≈7), the reaction mixture was stirred at room temperature for 2h. The suspension was centrifuged, and the solid collected was suspended in methanol (5 ml). The resulting solid was removed by centrifugation, and the filtrate was concentrated under reduced pressure to give 44 mg of the desired product as a beige solid (yield: 30%). UV-Vis spectroscopy: ε(319 nm): 8808 $M^{-1}cm^{-1}$ (water). Elemental Anal. Calc. for $C_{31}H_{30}EuF_3N_4O_7S\cdot(H_2O)_2$ (MW 847.6): C, 43.93; H, 4.04; N, 6.61; O, 16.99; S, 3.78 Found: C, 43.87; H, 4.00; N, 6.48; O, 17.04; S, 3.89

*{2-[(Pyridyl-2-ylmethyl)-amino]-cyclohexyl}-carbamic acid tert-butyl ester **6** and {2-[(Quinolyl-2-ylmethyl)-amino]-cyclohexyl}-carbamic acid tert-butyl ester **10*** : Compound **5** (0.670 g, 3.13 mmol) was added to a solution of 2-quinolinecarboxyaldehyde or 2-pyridinecarboxyaldehyde (3.13 mmol) in ethanol (35 ml) and stirred at room temperature for 12h. Sodium borohydride was slowly added to the mixture. The reaction was monitored by TLC ($SiO_2$, Cyclohexane:Ethyl acetate 7:3+ $NH_4OH$ 30% w/w) and after 4h the mixture was extracted twice with dichloromethane and the solvent removed under reduced pressure to give respectively the compound **6** and **10** as yellowish oils, in quantitative yield, which were used in next step without further purification.

*N-Pyridyl-2-ylmethyl-cyclohexane-1,2-diamine* (**7**) *and N-Quinolyl-2-ylmethyl-cyclohexane-1,2-diamine* (**11**): Compound **6** or **10** (3.13 mmol) was added to a trifluoroacetic acid 98% w/w (13 ml) and dichloromethane (40 ml) solution and stirred at room temperature for 12h. The solvent was removed under reduced pressure, and the obtained trifluoroacetate salt (≈3 g) was purified by cationic exchange chromatography (eluent: $NH_3$ 3M in MeOH) to give 398 mg (yield 61%) of the ligand **11**. $^1$H-NMR ($CDCl_3$) δ (ppm) 8.13 (d, J= 8.33 Hz, 1H), 8.08 (d, J= 8.56 Hz, 1H), 7.81 (d, J= 8.33 Hz,

1H), 7.71 (t, J= 7.74 Hz, 1H), 7.55-7.48 (m, 2H), 4.25 (dd, $J_{GEM}$= 14.55 Hz, 1H), 4.07 (dd, $J_{GEM}$= 14.55 Hz, 1H), 3.71 (m, 1H), 2.50 (m, 1H), 2.18 (m, 2H), 1.92 (m, 1H), 1.75 (m, 1H), 1.70 (m, 1H), 1.35-1.04 (m, 5H). $^{13}$C-NMR ($CDCl_3$) δ (ppm) 160.2, 148.2, 135.4, 129.0, 128.8, 127.3, 126.1, 125.1, 122.1, 57.1, 53.2, 52.1, 31.4, 28.9, 22.3. Elemental Anal. Calc. for $C_{16}H_{21}N_3$ (MW 255.4): C, 75.26; H, 8.29; N, 16.46 Found: C, 75.21 ; H, 8.22; N, 16.39

*Compound **7**:* Yield 38%. $^1$H-NMR ($CDCl_3$) δ (ppm) 8.52 (m, 1H), 7.62 (t, J= 7.54 Hz, 1H), 7.34 (d, J= 7.70 Hz, 1H), 7.13 (t, J= 5.90 Hz, 1H), 4.03 (dd, $J_{GEM}$= 14.09 Hz, 1H), 3.83 (dd, $J_{GEM}$= 14.09 Hz, 1H), 3.64 (m, 1H), 2.43 (m, 1H), 2.18 (m, 2H), 1.88 (m, 1H), 1.75 (m, 1H), 1.70 (m, 1H), 1.35-1.04 (m, 5H). $^{13}$C-NMR ($CDCl_3$) δ (ppm) 159.5, 149.0, 136.0, 123.5, 120.6, 57.8, 52.1, 31.5, 29.4, 22.3, 21.5. Elemental Anal. Calc. for $C_{12}H_{19}N_3$ (MW 205.3): C, 70.20; H, 9.33; N, 20.47 Found: C, 70.15 ; H, 9.19; N, 20.44

*N-picolyl-N,N',N'-trans-l,2-cyclohexylenediamine-tert-butyl triacetate* **(8)** and *N-quinolyl-N,N',N'-trans-l,2-cyclohexylenediamine-tert-butyl triacetate* **(12).** Under inert atmosphere, compound **7** or **11** (1.94 mmol, 1.20 mmol, respectively) was dissolved in an anhydrous acetonitrile (40 ml or 25 mL) solution of N,N-Diisopropylethylamine (6.8 mmol or 4.19 mmol,). Then, tert-Butyl 2-bromoacetate (6.8 mmol or 4.19 mmol) in anhydrous Acetonitrile (10 mL or 5 mL) was added dropwise. The reaction was monitored using TLC ($SiO_2$, Rf: 0.47, DCM:MeOH 95:5+ 0.5% $NEt_3$) and after 12 h, water (approx. 25 mL) was added and the reaction mixture was extracted twice with dichloromethane. The combined organic phases were dried on anhydrous $Na_2SO_4$ and the solvent was evaporated under reduced pressure to give 0.580 g of crude product which was purified by chromatography (on Silica gel, DCM/MeOH 95:5 + 0.5% Triethylamine, Rf: 0.47) giving rise to compounds **8** (yield 58%) and **12** (yield = 55%).

Compound **8**: $^1$H-NMR ($CDCl_3$) δ (ppm) 9.97 (d, J=6.56, 1H), 8.79 (d, J=7.91, 1H), 8.34 (t, J=7.91, 1H), 7.94 (t, J=6.56, 1H), 6.30 (dd, $J_{GEM}$= 17.64 Hz, 1H), 5.94 (dd, $J_{GEM}$= 17.64 Hz, 1H), 4.55 (dd, $J_{GEM}$= 16.93 Hz, 2H), 3.53 (m, 2H), 3.44 (dd, $J_{GEM}$= 16.93 Hz, 2H), 2.66 (m, 3H), 2.08 (m, 2H), 1.78 (m, 2H), 1.45 (s, 27H), 1.12 (m, 3H). $^{13}$C-NMR ($CDCl_3$) δ (ppm) 172.4, 171.0, 170.5, 159.4, 149.4, 136.0, 121.3, 123.0, 72.9, 73.3, 73.5, 57.3, 55.5, 55.3, 54.0, 54.2, 30.5, 30.1, 29.4, 27.3, 26.9, 22.2. Elemental Anal. Calc. for $C_{30}H_{49}N_3O_6$ (MW 547): C, 65.78; H, 9.02; N, 7.67; O, 17.53 Found: C, 65.70; H, 8.95; N, 7.73; O, 17.41

Compound **12**: $^1$H-NMR ($CDCl_3$) δ (ppm) 8.12 (m, 2H), 8.07 (d, 1H), 7.81 (d, J=7.92, 1H), 7.67 (t, J=7.71, 1H), 7.51 (t, J=7.29, 1H), 4.32 (dd, $J_{GEM}$= 13.79 Hz, 1H), 3.94 (dd, $J_{GEM}$= 13.79 Hz, 1H), 3.60 (m, 2H), 3.52 (m, 4H), 2.81 (m, 1H), 2.67 (m, 1H), 2.15 (m, 1H), 2.09 (m, 1H), 1.74 (m, 2H), 1.45 (s, 27H), 1.14 (m, 4H). $^{13}$C-NMR ($CDCl_3$) δ (ppm) 173.1, 172.9, 172.1, 160.2, 148.0, 134.0, 130.3, 127.5, 126.0, 124.7, 123.0, 74.5, 74.1, 73.3, 58.2, 57.4, 56.0, 55.3, 55.0, 54.1, 33.0, 32.3, 32.1,

28.1, 27.3, 22.8, 22.1. Elemental Anal. Calc. for $C_{34}H_{51}N_3O_6$ (MW 597.8): C, 68.31; H, 8.60; N, 7.03; O, 16.06 Found: C, 68.27; H, 8.51; N, 7.00; O, 15.97

*N-picolyl-N,N',N'-trans-l,2-cyclohexylenediaminetriacetic acid* (**$H_3$PyC3A, 9** as ammonium salt) and *N-quinolyl-N,N',N'-trans-l,2-cyclohexylenediaminetriacetic acid* (**$H_3$QC3A, 13** as ammonium salt). Compound **8** or **12** (1.12 mmol, 0.652 mmol, respectively) was added to an aqueous HCl (6 M, 22 ml or 13 ml) solution and stirred at ≈80°C for 12 h. After neutralization with NaOH, extraction with DCM was performed and the resulting aqueous solution was evaporated under reduced pressure. The solid was washed with ethanol for 1h at 80°C. Upon cooling, the suspension was filtered to remove all the insoluble inorganic salts and the resulting solution was evaporated under reduced pressure and the crude product was purified by ionic exchange chromatography to give the corresponding product **9** or **13**, (yield = 24% for **9** and 40% for **13**). Compound **9**: ESI-MS(Scan ES+; *m/z*): 468 (100%); 469 (20%) ($[Na_4(PyC3A)]^+$). Elemental Anal. Calc. for $C_{18}H_{34}N_6O_6$ (MW 430.5): C, 50.22; H, 7.96; N, 19.52; O, 22.30 Found: C, 50.18 ; H, 7.90; N, 19.47; O, 22.18.

Compound **13**: ESI-MS(Scan ES+; *m/z*): 513 (100%); 514(25%) ($[(NH_4)Na_3(QC3A)]^+$). Elemental Anal. $C_{22}H_{36}N_6O_6$ (MW 480.6): C, 54.99; H, 7.55; N, 17.49; O, 19.98 Found: C, 54.90 ; H, 7.46; N, 17.42; O, 20.01.

Eu(PyC3A) (**14a**) [and Tb(PyC3A) (**14b**)] has been synthesized as follows: Ligand **9** (60 mg, 0.140 mmol was partially dissolved in a mixture of 2-propanol:ethanol 1:1 (4 ml) by heating at ≈60°C. Then, europium(III) trifluoromethanesulfonate 98% (83.6 mg, 0.140 mmol) was added portion-wise and the pH of the solution was carefully adjusted to 7 by addition of KOH 2 M aq. The obtained suspension was stirred at room temperature for 12h. The collected solid (≈94 mg) was re-crystallized in methanol (≈10 ml) and $Et_2O$ (≈30 ml) solution to yield 70 mg (yield 95%) of a whitish solid (**14a**). UV-Vis spectroscopy: ε(265 nm): 3390 $M^{-1}cm^{-1}$ (water). ESI-MS(Scan ES+; *m/z*): 552 (100%); 550 (90%) ($[NaEu(PyC3A)]^+$). Elemental Anal. Calc. for $C_{18}H_{22}EuN_3O_6{\cdot}(H_2O)_2$ (MW 564.4): C, 38.31; H, 4.64; N, 7.45; O, 22.68 Found: C, 38.28; H, 4,54; N, 7.40; O, 22.51.

Ligand **9** (27 mg, 0.063 mmol) was dissolved in water (3 ml), then Terbium(III) chloride hexahydrate (23.5 mg, 0.063 mmol) was added portion-wise and the pH of the solution was carefully adjusted to 7 by addition of KOH 2M aq. The obtained solution was stirred at room temperature for 12h. The solvent was removed under reduced pressure and the residue was re-crystallized in methanol (≈2 ml) and $Et_2O$ (≈15 ml) solution yielding a white solid after centrifugation (34 mg of **14b**, quantitative yield). UV-Vis spectroscopy: ε(266 nm): 4008 $M^{-1}cm^{-1}$ (water). ESI-MS(Scan ES+; *m/z*): 558 (100%) ($[NaTb(PyC3A)]^+$). Elemental Anal. Calc. for $C_{18}H_{22}TbN_3O_6{\cdot}(H_2O)_2$ (MW 571.3): C, 37.84; H, 4.59; N, 7.35; O, 22.40 Found: C, 37.78; H, 4.50; N, 7.30; O, 22.37.

Eu(QC3A) (**15**) has been synthesized as follows: compound **13** (60 mg, 0.125 mmol) was partially dissolved in a mixture of 2-propanol:ethanol 8:2 (6 ml) at ≈ 60°C. Then, $Eu(CF_3SO_3)_3$ 98% (75 mg, 0.125 mmol) was added portion-wise followed by KOH 2M aq until pH ≈ 7. The obtained suspension was stirred at room temperature for 12h. The solid was removed under centrifugation, and the solution were dried under reduced pressure to give ≈112 mg of a white solid, which was re-crystallized in ethanol (≈10 ml) and $Et_2O$ (≈40 ml) solution, yielding a white solid after centrifugation (55 mg; yield 76%). UV-Vis spectroscopy: ε (319 nm) = 3725 $M^{-1}cm^{-1}$(water). ESI-MS(Scan ES+; *m/z*): 602 (100%); 600 (92%) ($[NaEu(QC3A)]^+$). Elemental Anal. Calc. for $C_{22}H_{24}EuN_3O_6\cdot(H_2O)_2$ (MW 614.4): C, 43.00; H, 4.59; N, 6.84; O, 20.83 Found: C, 42.97; H, 4.54; N, 6.74; O, 20.76.

*$^1$H-NMR spectroscopy*

Nuclear magnetic resonance (NMR) experiments were performed at 298.15 K using a 600 MHz Bruker Avance III spectrometer equipped with a triple resonance TCI cryogenic probe. Spectra were usually recorded in $CDCl_3$ and, unless otherwise noted, chemical shifts are expressed as ppm and referenced to the internal standard tetramethylsilane (TMS). One dimensional NMR spectra were recorded with 8 or 16 scans and a spectral width of 12019 Hz. All spectra were manually phased and baseline corrected using TOPSPIN 3.2 (Bruker, Karlsruhe, Germany). Chemical shift, multiplicity (s, singlet; d, doublet; t, triplet; m, multiplet; b, broad), coupling constants and integration area are reported.

*Elemental analysis*

Elemental analyses were carried out by using a EACE 1110 CHNOS analyzer.

*Potentiometric titrations*

The protonation constants of the ligands (bQcd (**3**), PyC3A (**9**) and QC3A (**13**)) were determined by acid-base potentiometric titrations. The titration cell was maintained at constant temperature (298.15 ± 0.1 K) using a circulatory bath. A computer-controlled potentiometer (Amel Instruments, 338 pH Meter) collected the electromotive force (emf) values measured by means of a combined glass electrode (Metrohm Unitrode 6.0259.100). Before each titration the electrode was calibrated by an acid-base titration with standard HCl and NaOH solutions and the carbon dioxide contamination in solution was checked by Gran's method.[29] Titrations were performed in duplicate on solutions containing the ligand (typical concentration around 0.9 mM for **3**, 0.6 mM for **9** and 0.7 mM for **13**)

and an excess of standard HCl by adding standard NaOH solution. The pH range was varied from an initial approximate value of 2.3 to about pH 11.5. All the solutions were prepared with ultrapure water (>18 MΩ cm) from a Milli-Q system (ELGA Purelab Option-Q) and the ionic strength (μ) was adjusted to 0.1 M by using appropriate amounts of NaCl (Sigma-Aldrich). Among 50-70 points were collected in each titration and processed with Hyperquad.[30]

*Spectrophotometric titrations*

The formation constants of all the L-Ln(III) complexes (L=**3, 9, 13**; Ln = Eu, Tb) were determined by UV-Vis spectrophotometric acid-base titrations.[31] A Varian Cary 50 instrument equipped with a fibre optic (optical path of 10 mm) was used. The wavelength range investigated was 240-300 nm for **9** and 275-355 nm for **3** and **13** in the same pH range and μ as in the potentiometry**.** The titration cell was maintained at T = 298.15 ± 0.15 K by means of a circulatory bath, and contained both the ligand (ligand **3**, 0.08 mM with Eu(III), 0.03 mM with Tb(III); ligand **9**, 0.13 mM with Eu(III), 0.15 mM with Tb(III); ligand **13**, 0.09 mM with both, Eu(III) and Tb(III)) and the Ln(III) (1:1 L:Ln(III) ratio, with a slight metal excess). The NaOH and HCl stock solutions were the same used during the potentiometric titrations. The stock solutions of Eu(III) and Tb(III) were prepared by dissolving their chloride hexahydrate salts (Sigma-Aldrich). The lanthanide content in the stock solutions was determined by EDTA titration, using xylenol orange as indicator.[32] Free acid concentrations in lanthanide solutions were checked by Gran's method.[29] Formation constants were calculated by simultaneous fit of the absorbance values at several wavelengths using HypSpec.[30]

*ESI-MS*

Electrospray ionization mass spectra (ESI-MS) were recorded with a Finnigan LXQ Linear Ion Trap (Thermo Scientific, San Jose, CA, USA) operating in positive ion mode. The data acquisition was under the control of Xcalibur software (Thermo Scientific). A MeOH solution of sample was properly diluted and infused into the ion source at a flow rate of 10 μL/min with the aid of a syringe pump. The typical source conditions were transfer line capillary at 275°C; ion spray voltage at 4.70 kV; sheath, auxiliary and sweep gas ($N_2$) flow rates at 10, 5 and 0 arbitrary units, respectively. Helium was used as the collision damping gas in the ion trap set at a pressure of 1 mTorr.

*DFT calculations*

As the paramagnetic Eu(III) and Tb(III) complexes are rather difficult to model computationally, the analogues of the diamagnetic Y(III) ion were studied. It has been shown that Y(III) complexes may serve as suitable models for the Eu(III) analogues,[33–36] consistently with the fact that its ionic radius differs from that of Eu(III) ion by about 0.05 Å [and less for Tb(III)]. Geometry optimizations of the $[Y(L)(H_2O)_n]$ complexes were carried out at DFT level in vacuum using the B3LYP exchange–correlation functional.[37,38] The 6-31+G(*d*) basis set was employed for the ligand atoms, while Y(III) ion was described by the quasi-relativistic small core Stuttgart-Dresden pseudopotential and the relative basis set.[39] This level of theory was previously demonstrated to provide correct geometries and thermochemical properties, maintaining the calculation feasible also with similar complex systems.[23,33] All final geometries were checked to be minima by vibrational analysis. Solvent effects were included by means of the PCM model.[40] All calculations were carried out with Gaussian16.[41]

The complexes studied were the *trans*-O,O and *trans-N,N* isomers of the Y(III) complexes ([Y(*trans*-O,O-bQcd)$(H_2O)_5]^+$ and [Y(*trans*-N,N -bQcd)$(H_2O)_5]^+$), as the c*is*-O,O, c*is*-N,N isomer was demonstrated to be much less stable in the case of bpcd.[33] As previously done[33] for the analogues with bpcd, five water molecules were initially placed near the metal ion. During the geometry optimization only two of them were retained in the first coordination sphere. Also in the case of the complexes with the triacetate ligands ([Y(PyC3A)$(H_2O)_3$] and [Y(QC3A)$(H_2O)_3$]) one water was always expelled from the starting structure to provide a final complex with only two inner sphere waters. Since the final number of coordinated water molecules was 2 in all cases, the $[Y(L)(H_2O)_2]$ complexes were considered for structural comparisons. The calculations have been performed on the two possible coordination geometries of the ligands (Figure S1) giving rise to [Y(*trans*-O,O-L)$(H_2O)_2$] and [Y(*trans*-N,O-L)$(H_2O)_2$] isomeric complexes. Andrea: dettagli sui calcoli degli addotti qui?

*Luminescence and decay kinetics*

Room temperature luminescence was measured with a Fluorolog 3 (Horiba-Jobin Yvon) spectrofluorometer, equipped with a Xe lamp, a double excitation monochromator, a single emission monochromator (mod. HR320) and a photomultiplier in photon counting mode for the detection of the emitted signal. All the spectra were corrected for the spectral distortions of the setup.

In decay kinetics measurements, a Xenon microsecond flashlamp was used and the signal was recorded by means of multichannel scaling method. True decay times were obtained using the convolution of the instrumental response function with an exponential function and the least-square-sum-based fitting program (SpectraSolve software package). The total quantum yields ($\Phi_{Tot}$) have been obtained by secondary methods described in the literature[42] by measuring the Visible emission

spectrum of quinine bisulfate in 1N $H_2SO_4$ solution, a fluorescence quantum yield reference sample ($\Phi$ = 54.6%). $\Phi_{Tot}$ for the complexes has been calculated by $[(A_s \cdot F_u \cdot n^2)/( A_u \cdot F_s \cdot n_o^2)] \cdot \Phi_s$ equation; were: u subscript refers to unknown and s to the standard and other symbols have the following meanings: $\Phi$ is quantum yield, A is absorbance at the excitation wavelength, F the integrated emission area across the band and n's are respectively index of refraction of the solvent containing the unknown (n) and the standard ($n_0$) at the sodium D line and the temperature of the emission measurement (see ESI, figures S15-S20).

*Luminescence sensing of $HCO_3^-$*

The binding interactions between hydrogen carbonate and the Eu(III) complexes were studied using the double reciprocal plot following the Benesi-Hildebrand equation[43] adapted to the values of the asymmetry ratio (*R*) of the Eu(III) emission spectra:

$$\frac{R_0}{R - R_0} = \frac{R_0}{R_\infty - R_0} + \frac{R_0}{\{K(R_\infty - R_0)[HCO_3^-]^n\}}$$

where $R_0$, $R$, and $R_\infty$ are the asymmetry ratio of Eu(III) in the complexes considered in the absence of hydrogen carbonate, at an intermediate hydrogen carbonate concentration and at a concentration of complete interaction, respectively. In the above equation, *K* is the binding constant and *n* the number of hydrogen carbonate anion bound to the metal center and $[HCO_3^-]$ is the hydrogen carbonate concentration. The models have been validated by the statistical tests present in the MS-Excel cEST program here adapted to treat fluorescence data.[44]

## Results and discussion

*Synthesis*

The synthesis of the ligands and the relative Ln(III) complexes discussed in this paper are presented in schemes 1 and 2.

For the synthesis of the $C_1$-symmetric ligands **9** and **13**, we exploit the straightforward chemistry of the t-Butyloxycarbonyl (BOC) protective group. In this context, the derivative **5** (scheme 2) can be obtained in good yield as previously reported.[45] All the ligands (**9** and **13**) and the relative Ln complexes (**14** and **15**) have been obtained in good yield and with a high degree of purity (see experimental section for details)..

The chlorides of the cationic complexes Eu(bpcd) and Tb(bpcd) were synthesized as reported previously.[33] The synthesis of **1** (scheme 1) has already been reported previously,[24] as well as the synthesis of **5**.[45]

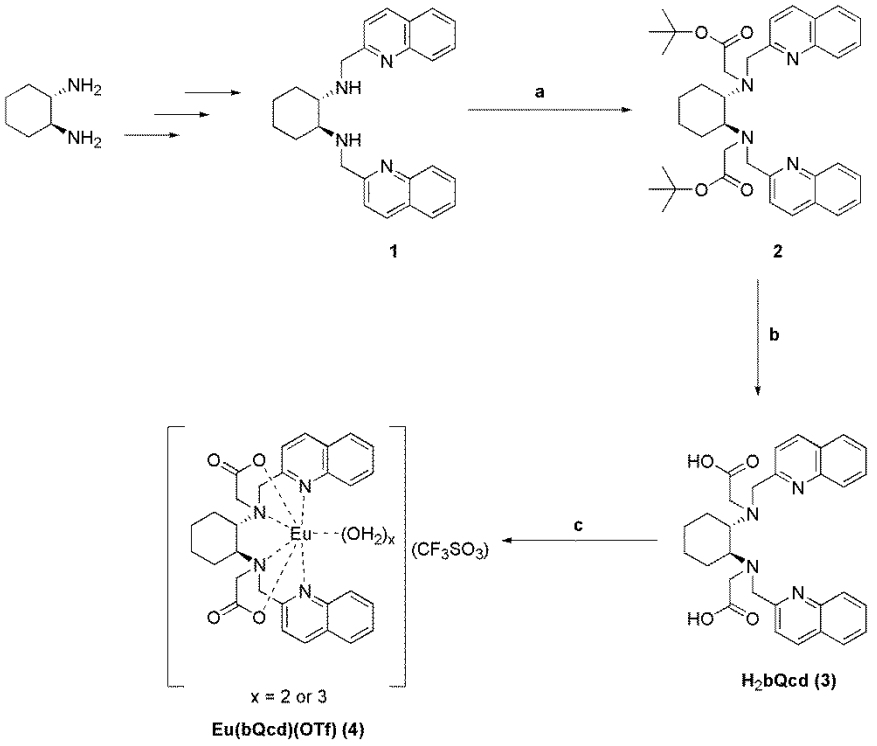


**Scheme 1.** Synthetic protocol for the synthesis of $H_2$bQcd (**3**) and Eu(bQcd)($CF_3SO_3$) (**4**).(a) tert-butyl bromoacetate 3 eq, $K_2CO_3$ 3.2 eq, MeCN, room temperature, 12 h; (b) HCl 6 M aq. 80°C, 12 h; (c) Eu($OTf)_3$ 1 eq, 2-propanol, room temperature, 12 h.

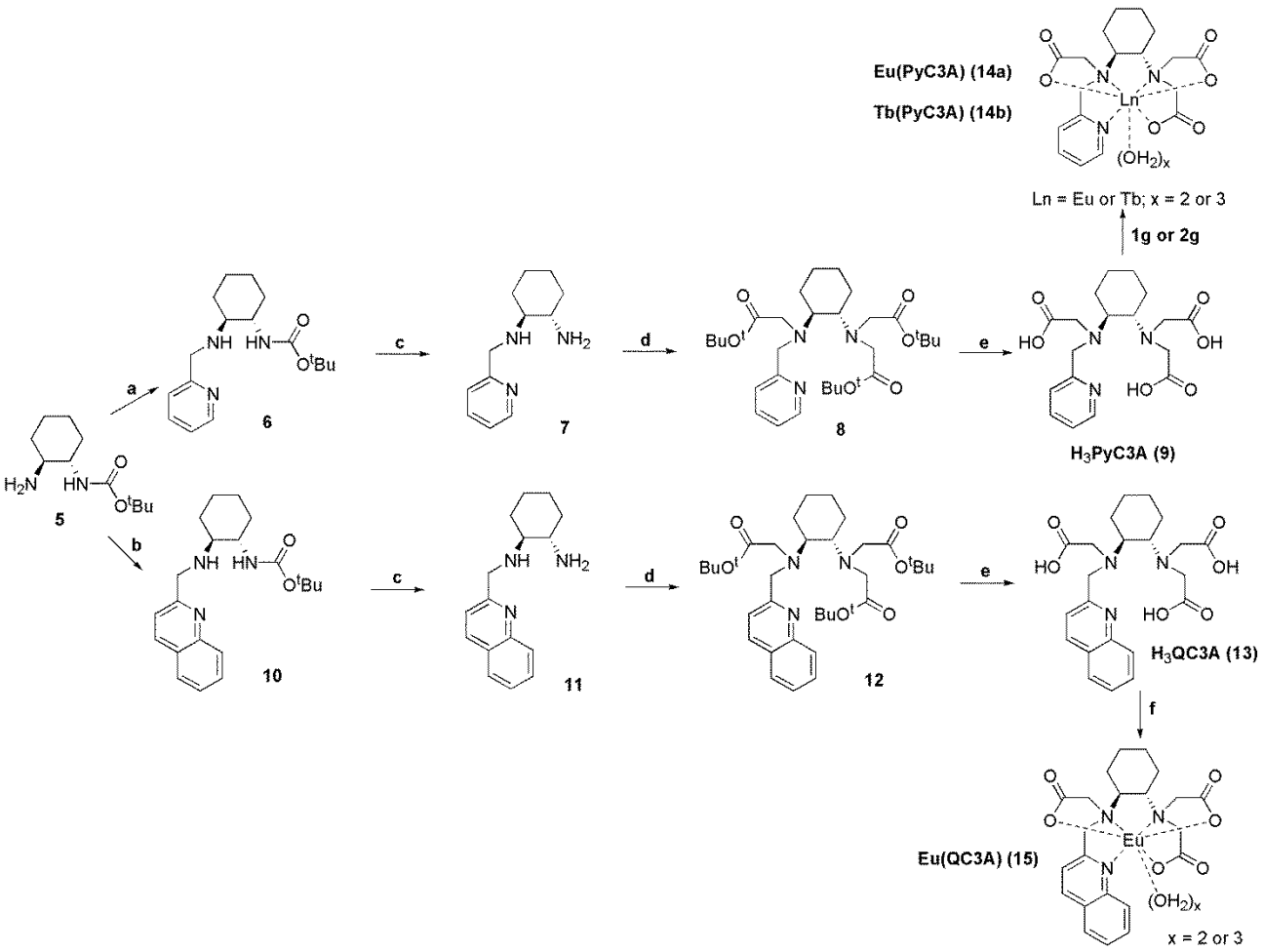


**Scheme 2.** Synthetic protocol for the synthesis of the ligands $H_3$PyC3A (**9**), $H_3$QC3A (**13**), the Eu(III) complexes Eu(PyC3A) (**14a**), Eu(QC3A) (**15**) and the Tb(III) complex Tb(PyC3A) (**14b**). (a) Pyridine-2-carbaldehyde 1eq, absolute ethanol, room temperature, 12 h; $NaBH_4$ 1.2 eq, MeOH, room temperature, 12 h; (b) Quinoline-2-carbaldehyde 1eq, absolute ethanol, room temperature, 12 h; $NaBH_4$ 1.2 eq, MeOH, room temperature, 12 h (c) Trifluoroacetic Acid:dichloromethane (1:3), room temperature, 12 h; (d) tert-butyl bromoacetate 3.5 eq, N,N-Diisopropylethylamine 3.5 eq, MeCN, room temperature, 12 h; (e) HCl 6 M aq. 80°C, 12 h; (f) $Eu(OTf)_3$ 1 eq, 2-propanol:ethanol (8:2), room temperature, 12 h; (1 g) $Eu(OTf)_3$ 1 eq, 2-propanol:ethanol (1:1), room temperature, 12 h (2 g) $TbCl_3 \cdot 6H_2O$ 1 eq, water, room temperature, 12 h.

*Protonation constants*

The best fit of the potentiometric data was obtained for all three ligands (**3**, **9** and **13**) when four protonated species were considered. The obtained log$K_n$ are reported in Table 1 along with the constants for similar ligands containing the chiral DACH backbone: bpcd,[33] PyC3A (**9**)[46] and CDTA[46]

(1,2-cyclohexanediaminetetraacetic acid). The titration curves for ligand **3, 9 and 13** are displayed in Figure S2, S3 and S4 respectively, together with the speciation plots calculated by using the protonation constants in Table 1.

**Table 1** Protonation constants ($\log K_n$, $K_n = [LH_n]/([H]\cdot[LH_{n-1}])$ of the ligands **3**, **9** and **13** with their confidence intervals (T = 298.15 K and μ = 0.1 M NaCl,). Additional protonation data for similar ligands are also reported. Charges omitted for clarity.

| | **bQcd (3)** | **PyC3A (9)** | **QC3A (13)** | **bpcd[a]** | **PyC3A[b]** | **CDTA[b]** |
|---|---|---|---|---|---|---|
| **log$K_1$** | 9.37 ± 0.03 | 10.26 ± 0.02 | 10.53 ± 0.03 | 9.72 ± 0.02 | 10.16 ± 0.02 | 9.43 ± 0.02 |
| **log$K_2$** | 5.85 ± 0.07 | 6.33 ± 0.07 | 6.29 ± 0.09 | 5.87 ± 0.07 | 6.39 ± 0.04 | 6.01 ± 0.02 |
| **log$K_3$** | 3.46 ± 0.10 | 3.67 ± 0.11 | 3.60 ±0.16 | 2.94 ± 0.12 | 3.13 ± 0.03 | 3.68 ± 0.02 |
| **log$K_4$** | 1.79 ± 0.31 | 2.01 ± 0.14 | 2.81 ± 0.16 | 2.22 ± 0.17 | - | 2.51 ± 0.05 |

a) ref.[33] ; b) ref.[46], μ = 0.15 M NaCl

The log$K$ values reported in Table 1 indicate that two fairly strong acidic and two weakly acidic sites are present. In particular, the values for the first protonation constant of the ligands **3**, **9** and **13** (Table 1) are in agreement with those reported for tertiary amines (log$K$ ~ 6.9-10.7, depending on the substituents).[47] This suggests that the first protonation constant can be assigned to an aliphatic amino group, as previously reported for bpcd[33] and CDTA.[48]

Spectrophotometric acid-base titrations were performed in order to study the species distribution of the ligand as a function of the pH. The molar absorbance ($\varepsilon_\lambda$) variations are reported in Figure 2, for the ligand **3.**

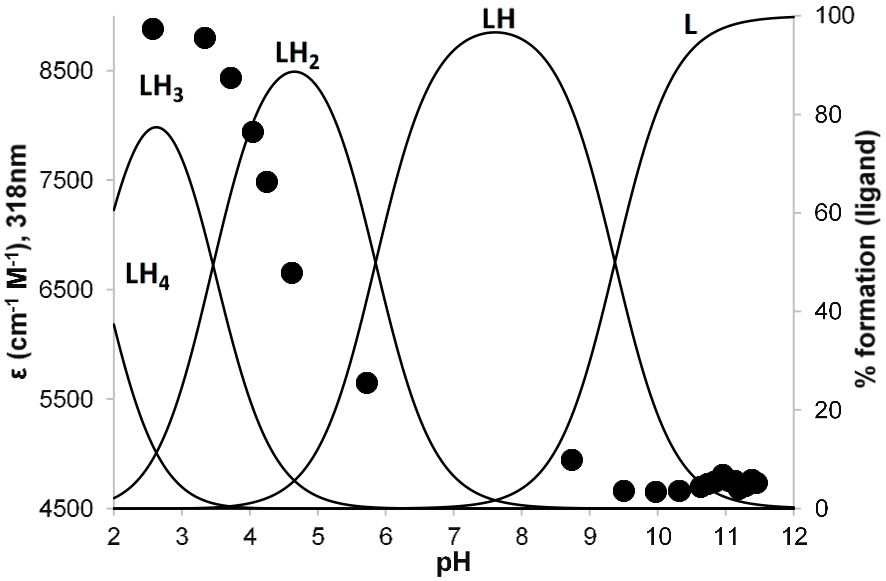


**Figure 2** Species distribution of the ligand **3** (L) along with the molar absorbance values at λ= 318 nm obtained by acid-base spectrophotometric titration (T = 298.15 K, μ = 0.1 M NaCl). The speciation was calculated by using the fitted protonation constants (table 1) and the concentration of **3** ([L] = 0.09 mM $dm^{-3}$). Charges omitted for clarity.

Similar plots are reported for the ligands **9** and **13** in figures S5 and S6. For the ligand **3** (Figure 2), $\varepsilon_\lambda$ is nearly constant in the range 11-8.5 and then increases below pH~8.5 with the formation of the bi- and tri-protonated species ($\log K_2$ = 5.85, $\log K_3$ = 3.46). This change is related to the protonation of the quinoline moieties, and is compatible with the protonation constant of quinoline ($\log K$ = 4.97).[49] The $\varepsilon_\lambda$ values of **9** and **13** increase below pH ~ 8 together with the formation of $LH_2$ species, presumably related to the protonation of the pyridine and quinoline moieties. The associated protonation values ($\log K_2$ = 6.33 for **9**, $\log K_2$ = 6.29 for **13**) are in line with the protonation constants of 2-methylpyridine (picoline) and quinoline ($\log K$ = 6.06 for picoline, $\log K$ = 4.97 for quinoline).[49,50] The remaining protonation constants ($\log K_4$ for **3**, $\log K_3$ and $\log K_4$ for **9** and **13**) could be ascribed to acetate moieties.[51]

*Ln(III) complex formation*

The formation constants of the Eu(III) and Tb(III) complexes with the ligands **3**, **9** and **13** were determined by acid-base spectrophotometric titration. In Figure S7 the absorbance changes upon addition of base to equimolar solutions of Eu(III) and the ligands **9** and **13** are shown. The spectra for the complexes containing the same chromophore are very similar (Figure S8).

In Figure 3, the speciation diagram for each studied Eu(III) complex along with the $\varepsilon\lambda$ changes for quinoline- ($\lambda$ = 318 nm) and pyridine- ($\lambda$ = 260 nm) based ligands are reported as a function of pH. The same plots for the Tb(III) complexes are very similar to its Eu(III) analogues and are reported in Figure S9. In all plots, the formation of the complex is accompanied by a steep decrease of $\varepsilon\lambda$.

The best fit of the spectrophotometric data has been obtained when only the ML species was considered and the formation constants obtained for Eu(III) and Tb(III) are reported in Table 2 along with those available for similar ligands for comparison. According to this model, at pH = 7.4 the ML species is largely predominant in all cases (>99%).

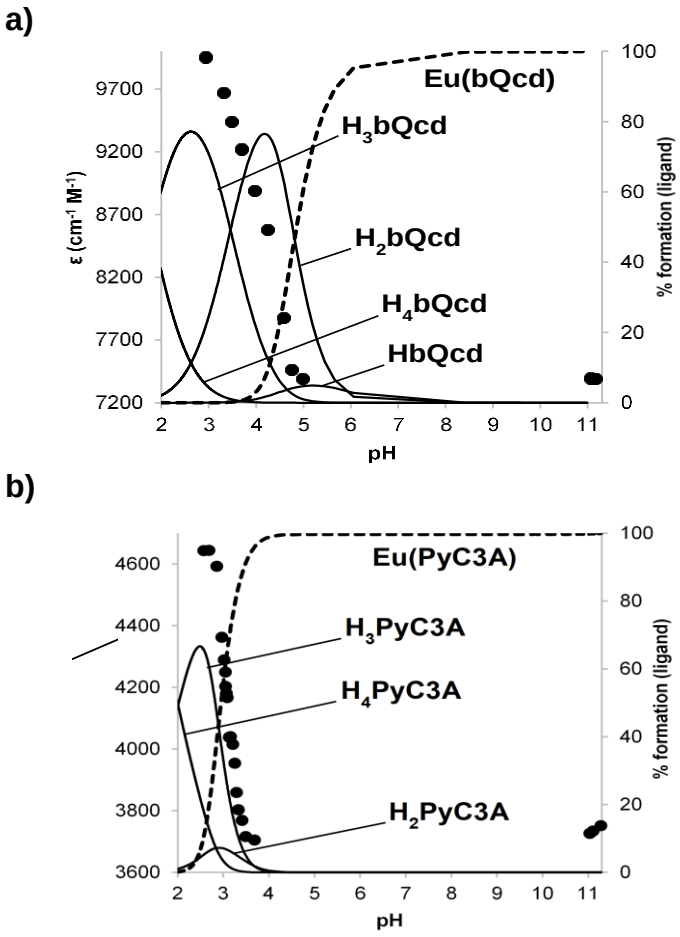

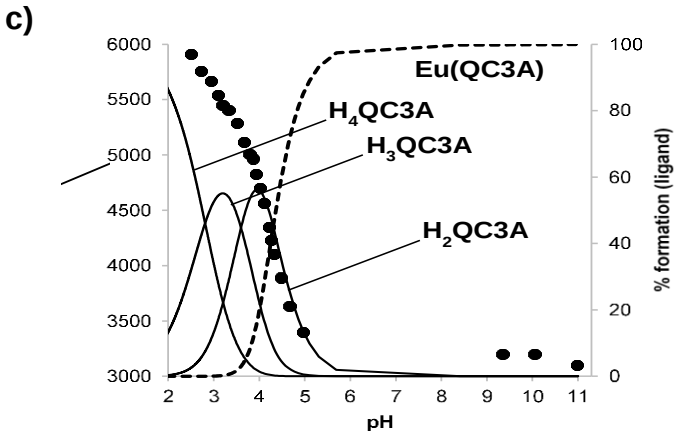


**Figure 3.** Species distribution of the complexes for the ligands a) **3** (0.08 mM), b) **9** (0.13 mM) and c) **13** (0.09 mM) with Eu(III) (ratio 1:1 M:L, with a little excess of metal), along with the molar absorbance values at λ=318 nm (for the ligands **3** and **13**) and λ=265 nm (for ligand **9**) obtained by acid-base spectrophotometric titration at T = 298.15K and μ = 0.1 M. Charges and negligible species (below 5%) omitted for clarity.

**Table 2** Formation constants (log*β*) complexes of the ligands **3**, **9** and **13**) with Eu(III) and Tb(III) at T = 298.15 K and μ = 0.1 M NaCl. Other similar complexes have been added for comparison. Charges omitted for clarity.

| Complex | bQcd (3) | PyC3A (9) | QC3A (13) | bpcd[a] | bped[b] | PEDTA[c] | CDTA[d] |
|---|---|---|---|---|---|---|---|
| **Eu(III)L** | 9.97 ± 0.08 | 15.682 ± 0.009 | 12.55 ± 0.16 | 11.19 ± 0.32 | - | - | 19.6 |
| **Eu(III)L(OH)** | - | - | - | 2.18 ± 0.57 | - | - | - |
| **Tb(III)L** | 9.80 ± 0.13 | 15.70 ± 0.02 | 12.08 ± 0.28 | 11.36 ± 0.15 | - | - | 20.0 |
| **Tb(III)L(OH)** | - | - | - | 2.04 ± 0.33 | - | - | - |
| **Gd(III)L** | - | - | - | - | 12.37 | 15.56 | 19.6 |
| **Gd(III)L(OH)** | - | - | - | - | 2.1 | - | - |

a) ref.[33]; b) ref.[52], μ = 0.16 M NaCl; c) ref.[53]; d) ref. [54]

As expected on the basis of the strong oxophilicity of Ln(III) ions,[55] the stability constants for the triacetate ligands [PyC3A (**9)** and QC3A (**13)**] are higher than their diacetate analogues [bpcd and bQcd (**3)** respectively]. Besides, the stability constants of the Ln(III) complexes with the quinoline-substituted ligands (**3** and **13**) are lower than for their pyridine analogues (bpcd and **9,** respectively). This result could be due to a weaker interaction of the quinoline moieties with respect to the pyridine ones and also to the increased steric hindrance. In the perspective of *in vitro* application experiments,

the values of these formation constants appear promising, in particular for triacetate-based ligands (**9** and **13**) whose stability is close to that of macrocyclic ligands possessing similar coordination ability and already employed in molecular imaging applications (*i.e.* DO3A derivatives with log$\beta$ values in the 18-21 range).[56]

Molecular models obtained by DFT calculations show that Y(III) is 8-fold coordinated in all cases and additional water molecules were expelled in the second-sphere as can be seen from the minimum energy structures in Figure S10. On this basis, further geometry optimizations were performed on the $[Y(L)(H_2O)_2]$ complexes in presence of PCM water. The increase of steric crowding when passing from pyridine- to the quinoline-substituted ligands can be clearly seen in Figure 4.

From the obtained bond distances (Table 3) it emerges that the substitution of pyridine by quinoline has nearly no effect on the Y(III)-$O_{acetate}$ bonds (average variation, $\Delta Py \rightarrow Q \sim -0.001$ and +0.005 Å for the di- and tri-acids, respectively), and also the Y(III)-$N_{amine}$ distances are marginally affected ($\Delta Py \rightarrow Q \sim -0.019$ and -0.006 Å). It can be noted also that Y(III)-$O_{water}$ bonds are slightly longer in the pyridine triacid isomers as it could be expected on the basis of the decreased charge on the metal ion, while in the quinoline complexes they are only slightly affected. However, the most remarkable finding is that the average Y(III)-$N_{heterocycle}$ bond distance increases significantly ($\Delta Py \rightarrow Q \sim +0.11$ Å), indicating the weaker interaction of the quinoline with respect to pyridine ligands with the metal ion; this possibly contributes to the drop of stability of the quinoline complexes with respect to the pyridine analogues (on average ~1.4 and 3.4 log units for the di and tri-acetate ligands). However, it is expected that quinoline has also a notable impact on the solvation properties of the complex which often have a strong influence on the stability.

**Table 3** Selected bond distances (Å) of the complexes in Figure 4.

| Complex | Y-$O_{acetate}$ | Y-$N_{amine}$ | Y-$N_{heterocycle}$ | Y-$O_{water}$ |
|---|---|---|---|---|
| $[Y(trans\text{-O,O bpcd})(H_2O)_2]^+$ | 2.262 | 2.550 | 2.525 | 2.448 |
| $[Y(trans\text{-N,N bpcd})(H_2O)_2]^+$ | 2.292 | 2.610 | 2.503 | 2.492 |
| $[Y(trans\text{-O,O bQcd})(H_2O)_2]^+$ | 2.268 | 2.557 | 2.661 | 2.464 |
| $[Y(trans\text{-N,N bQcd})(H_2O)_2]^+$ | 2.284 | 2.567 | 2.594 | 2.482 |
| $[Y(trans\text{-O,O PyC3A})(H_2O)_2]$ | 2.286 | 2.568 | 2.550 | 2.474 |
| $[Y(trans\text{-N,O PyC3A})(H_2O)_2]$ | 2.300 | 2.595 | 2.546 | 2.539 |
| $[Y(trans\text{-O,O QC3A})(H_2O)_2]$ | 2.286 | 2.574 | 2.654 | 2.458 |
| $[Y(trans\text{-N,O QC3A})(H_2O)_2]$ | 2.290 | 2.576 | 2.642 | 2.478 |

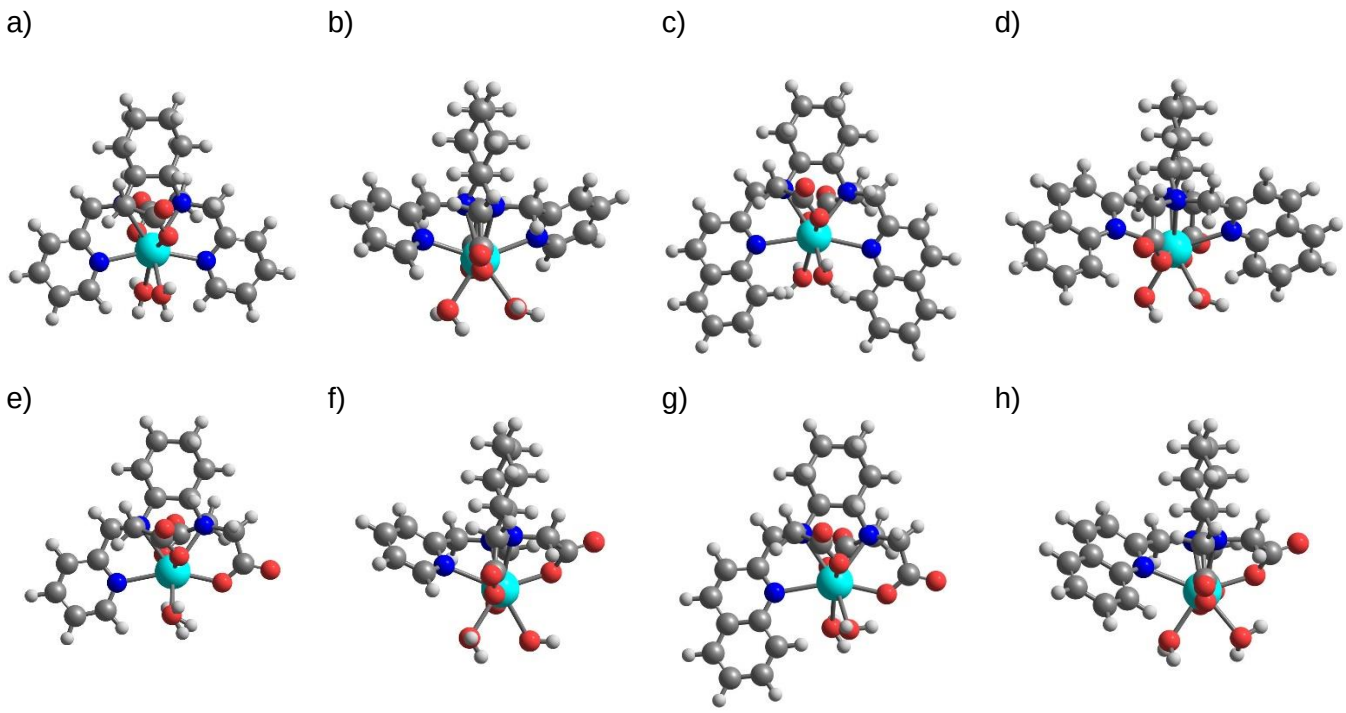


**Figure 4**. Minimum energy structures of (a) [Y(*trans*-O,O-bpcd)$(H_2O)_2]^+$; (b) [Y(*trans*-N,N-bpcd)$(H_2O)_2]^+$; (c) [Y(*trans*-O,O-bQcd)$(H_2O)_2]^+$; (d) [Y(*trans*-N,N-bQcd)$(H_2O)_2]^+$; (e) [Y(*trans*-O,O-PyC3A)$(H_2O)_2]^+$; (f) [Y(*trans*-N,O-PyC3A)$(H_2O)_2]^+$; (g) [Y(*trans*-O,O-QC3A)$(H_2O)_2]^+$; (h) [Y(*trans*-N,O-QC3A)$(H_2O)_2]^+$.

*Luminescence*

Excitation spectra of the complexes **4**, **14a**, **15** and Eu(bpcd)Cl dissolved in water upon monitoring the $^5D_0 \rightarrow ^7F_2$ transition of Eu(III) ($\lambda_{em}$ = 612-615 nm) are shown in the Figures 5 and 6 (left). In the case of Tb(III) complex **14b**, the excitation spectrum has been recorded monitoring the $^5D_4 \rightarrow ^7F_5$ transition of Tb(III) ($\lambda_{em}$ = 545 nm, Figure 6). As all the spectra are superimposable with the corresponding absorption ones, a ligand to metal energy transfer mechanism works in all the complexes under investigation. As already observed[33] the pyridine ring is capable to sensitize both Eu(III) and Tb(III) luminescence. On the other hand, the quinoline ring effectively sensitizes only Eu(III) ion.

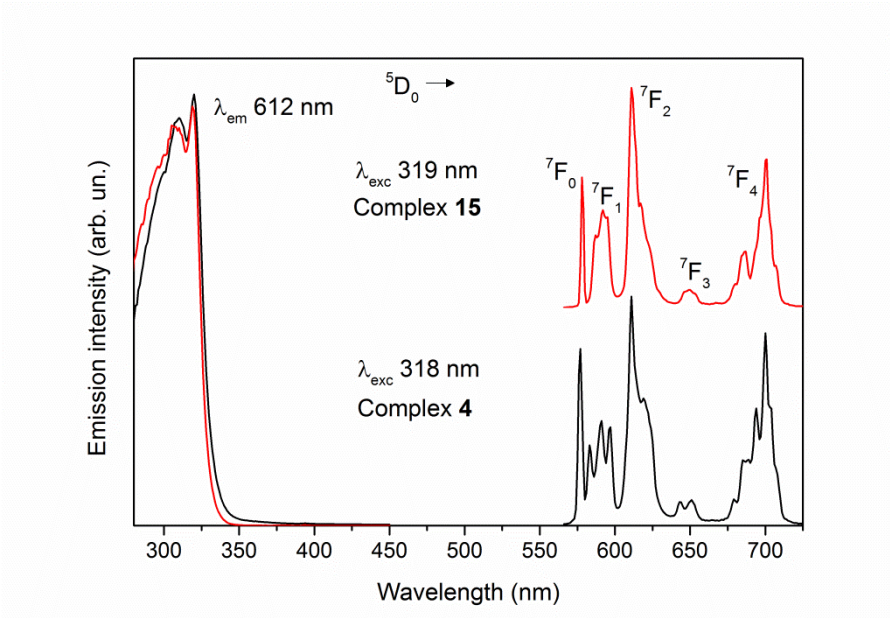


**Figure 5.** Luminescence excitation spectra (left) and emission spectra (right) of Eu(III) complex **4** and **15** in water solution ($10^{-4}$ M) at 298 K.

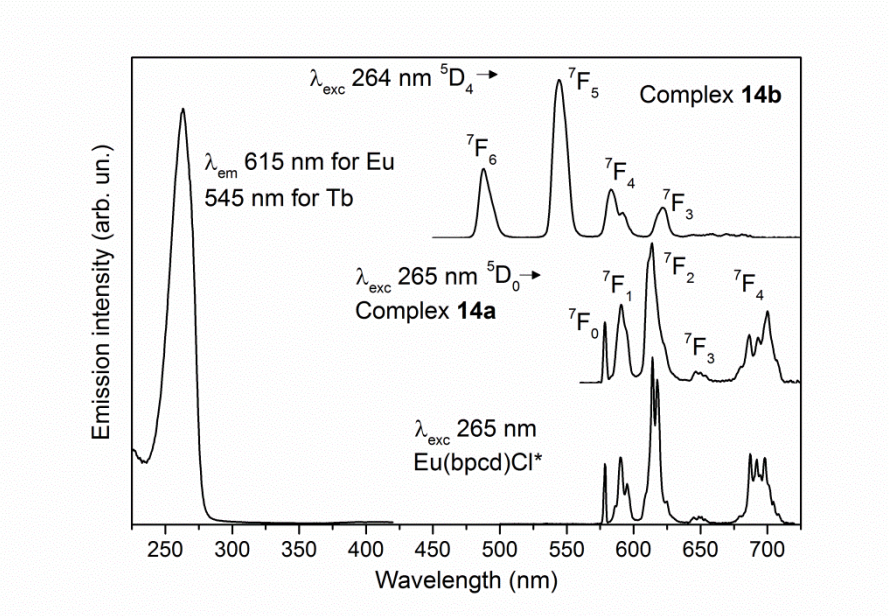


**Figure 6.** Luminescence excitation spectra (left) and emission spectra (right) of Eu(III) complex **14a** and Eu(bpcd)Cl and Tb(III) complex **14b** in water solution ($10^{-4}$ M) at 298 K. *data from ref. [33].

As far as the luminescence emission spectra are concerned (Figures 6 and 7, right), the typical Eu(III) or Tb(III) luminescence originating from *f-f* transitions is clearly detected for all the complexes. Upon excitation of the pyridine ring ($\lambda_{exc}$ = 265 nm) the complexes **14a** and Eu(bpcd)Cl showed a visual red luminescence while the complex **14b** a green one. Upon excitation of the quinoline ring ($\lambda_{exc}$ = 319 nm) a red luminescence is detected for the complexes **4** and **15**. In all the Eu(III) emission spectra, the hypersensitive $^5D_0 \rightarrow {}^7F_2$ transition dominates the spectrum and one strong $^5D_0 \rightarrow {}^7F_0$ band is also detected (in particular in the case of quinoline-based complexes). All this is compatible with the presence of emitting species where the point symmetry of Eu(III) deviates from the inversion symmetry and is characterized by an axial character.[57] The $C_n$, $C_{nv}$ or $C_s$ are the only possible point symmetry in the presence of sizeable intensity of the $^5D_0 \rightarrow {}^7F_0$ transition[57] even though in our case, the $C_s$ symmetry can be ruled out due to the presence of the chiral ligand.

The luminescence decay curves of the $^5D_0$ and $^5D_4$ excited states of Eu(III) and Tb(III), respectively were recorded in aqueous solution for all the complexes under investigation; in Figure S12 we report only a representative selection. All the curves are well fitted by a single exponential function and the observed lifetimes, in water and deuterium oxide, are reported in Table 4, together with the values of the hydration number ($q$), the radiative lifetime ($\tau_{rad}$), the intrinsic ($\Phi_{Ln}$), the total ($\Phi_{Tot}$) quantum yields and the efficiency of the sensitization of the lanthanide luminescence by the ligand ($\eta_{sens}$). The hydration number is the number of water molecule in the close proximity of the metal ion and can be calculated by means of the Horrock's equation[58–60] that is based on the values of $\tau_{obs}$ in $H_2O$ and $D_2O$.

**Table 4.** Observed and radiative excited state lifetimes (ms) for Eu(III) and Tb(III) complexes along with the number of water molecules ($q$) obtained from data fitting. Intrinsic ($\Phi_{Ln}$), total ($\Phi_{Tot}$) quantum yields and $\eta_{sens}$ are also reported. a) estimated from the analysis of the Eu(III) emission spectra by using the formula reported by Werts et al.[61] b) calculated by $\tau_{rad} = \tau_{obs} / \Phi_{Ln}$; $\tau_{obs}$ and $\Phi_{Ln}$ have been determined in $H_2O$. c) estimated in aqueous solution thanks to the formula $\tau_{obs}/\tau_{rad}$. d) determined by using the reference standard.

| Complex | $\tau_{obs}$ | | $\tau_{rad}$ | $q$ | $\Phi_{Ln}$(%) | $\Phi_{Tot}$(%) | $\eta_{sens}$(%) |
|---|---|---|---|---|---|---|---|
| | $H_2O$ | $D_2O$ | | | | | |
| Eu(bpcd)Cl | 0.30(1) | 1.70(1) | 3.00[a] | 2.7(1) | 10.0[c] | 6.1 | 61 |
| Eu(bQcd)Cl | 0.29(1) | 1.68(1) | 3.22 [a] | 2.8(1) | 9.0 [c] | 2.6 | 29 |
| Eu(PyC3A) | 0.33(1) | 3.56(1) | 3.66 [a] | 2.7(1) | 9.0 [c] | 5.67 | 63 |
| Eu(QC3A) | 0.33(1) | 2.15(1) | 3.34 [a] | 2.5(1) | 9.9 [c] | 4.0 | 40 |
| Tb(bpcd)Cl | 0.94(1) | 2.15(1) | 5.98 [b] | 2.6(5) | 15.7 [d] | 10.0 | 64 |
| Tb(PyC3A) | 1.16(1) | 3.53(1) | 6.86 [b] | 2.4(5) | 16.9 [d] | 11.2 | 66 |

It is worth to be noted that the number of water molecules in the inner coordination sphere of the metal ion in each complex is, in practice, the same (around 2.5). This result seems to be in partial agreement with the DFT structures reported in Figure 6 where always two water molecules are retained in the first coordination sphere of the metal ion. Nevertheless, as already observed for the complexes Eu(bpcd)Cl and Tb(bpcd)Cl, this is compatible with the presence of an equilibrium in solution interconverting two species having one 6-fold coordinating ligand molecule and a different number of water molecules (2 or 3) in the inner coordination sphere of the metal ion.[33] In addition, it has to be reminded that the hydration number ($q$), calculated by the Horrock's equation, is also slightly sensitive to the presence of water molecules in the outer coordination sphere.[58]

The intrinsic quantum yield of the lanthanide ion ($\Phi_{Ln}$), defined by number of emitted/absorbed photons, when lanthanide ions is directly excited, is around 10% and 16% for the Eu(III) and Tb(III) complexes, respectively (Table 4). The higher values of the intrinsic quantum yield for the Tb(III)-based complexes is due to the energy gap between the emitting level and the lower lying ones, that is bigger in the case of Tb(III) so as to limit the multiphonon relaxation process. On the other hand, to estimate $\eta_{sens}$, we need to know the total quantum yield ($\Phi_{Tot}$), that is defined by the number of photons emitted by the lanthanide ion/number of photons absorbed by the ligand. Since, $\Phi_{Tot} = \eta_{sens} \cdot \Phi_{Ln}$, then $\eta_{sens} = \Phi_{Tot} / \Phi_{Ln}$. The values of $\Phi_{Tot}$ for all the complexes have been determined by using a

reference standard of known quantum yield (quinine bisulfate; Φ = 54.6%; see experimental section for details). The obtained $\eta_{sens}$ is in the 60-70% range for all Eu(III) and Tb(III) complexes containing the pyridine chromophore, whilst the Eu(III) complexes containing the quinoline fragment show a significantly lower sensitization efficiency (in particular for Eu(bQcd)OTf, $\eta_{sens}$ = 29%). This seems to be related to the longer Y-$N_{heterocycle}$ bond distances found by DFT calculations, in the case of quinoline-based complexes. In this context, it is useful to remember that the probability of the energy transfer from an antenna ligand (S = sensitizer) to a metal ion (A = acceptor) is strongly dependent on the S-A distance, for both the most common energy transfer processes taking place in lanthanide-based complexes (dipole-dipole and exchange mechanisms).[62] In particular, the longer is the distance, the lower is the energy transfer probability and the sensitization efficiency. The seemingly low total quantum yields ($\Phi_{Tot}$ in the 3-11% range) must be reassessed in the light of the following statements: *i)* The quantum yield of many lanthanide and d-block compounds used for cellular imaging is in the 4-10% range;[63,64] *ii)* the total quantum yield of our complexes, is expected to grow upon interaction of the complex with a target analyte thanks to the concomitant displacement of water molecules from the metal ion. For these reasons, we believe that the class of complexes under investigation can be considered a promising family of optical probes for sensing application.

*Sensing of $HCO_3^-$*

As can be seen from the inspection of the Figure 7, the intensity of the $^5D_0 \rightarrow {}^7F_0$ and $^5D_0 \rightarrow {}^7F_2$ Eu(III) transitions are significantly affected by the addition of the hydrogen carbonate ion to the complex **14a** (chosen as representative example). As it is reasonable to assume that $HCO_3^-$ anion is capable to coordinate the Eu(III) ion, displacing the water molecules from the inner coordination sphere, we can claim that the interaction between Eu(III) and the target anion produces an increase of the intensity of $^5D_0 \rightarrow {}^7F_2$ transition and a decrease of intensity of the $^5D_0 \rightarrow {}^7F_0$ one. This means that during the titration with $HCO_3^-$, the geometry of the Eu(III) environment is undercoming a change in symmetry. In fact, the values of the asymmetry ratio:

$$R = \frac{I(^5D_0 \rightarrow {}^7F_2)}{I(^5D_0 \rightarrow {}^7F_1)}$$

indicative of the degree of asymmetry of the coordination polyhedron around the Eu(III) ion, increase upon addition of the anion.

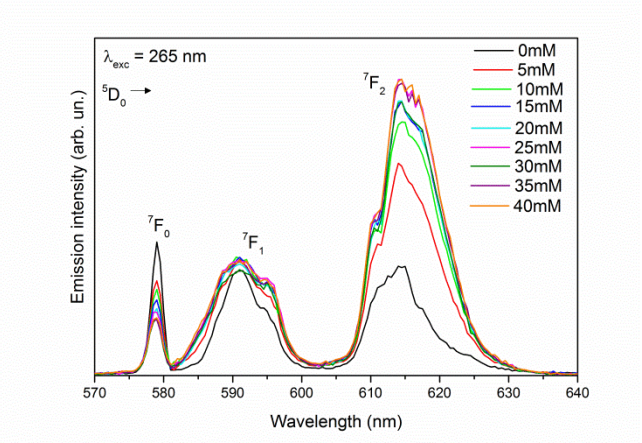


**Figure 7.** Eu(III) luminescence emission spectra of the complex **14a** (limited to 570-640 nm range) upon addition of hydrogen carbonate ion. The concentration of the anion is reported.

The value of *R* during the titration with hydrogen carbonate also increases for all the Eu(III) complexes under investigation (Figure 8).

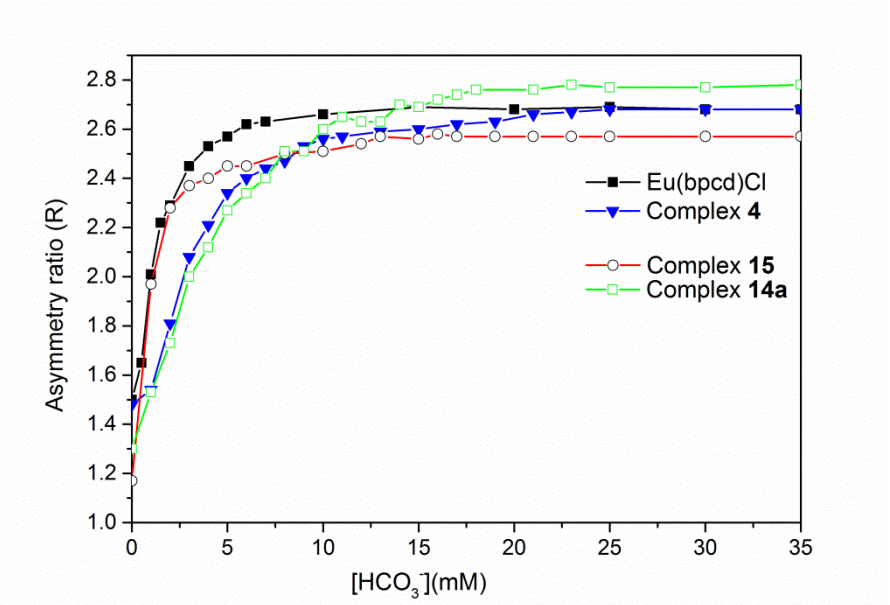


**Figure 8.** Asymmetry ratio (R) for the Eu(III) complexes *vs.* [$HCO_3^-$] concentration plots. The employed ligands are reported in each plot (reference labels in Figure 1).

In all cases, a logarithmic-like trend is observed, and an asymptote is reached after the addition of 10 mM of anion for Eu(III) complex with bpcd ligand (Figure 8). On the other hand, the asymptotic value is reached only after the addition of hydrogen carbonate at 15-20 mM, in the case of all the other complexes [Eu(bQcd)OTf, Eu(PyC3A) and Eu(QC3A)]. The sensitivity of the optical response to the $HCO_3^-$ concentration can be qualitatively evaluated by analyzing the slope of the graph in the

range of biological interest where the hydrogen carbonate concentration is related to serious metabolic acidosis (0-10 mM). As can be seen in figure 8, Eu(bpcd)Cl and Eu(QC3A) (**15**) complexes show the best sensitivity. The binding interactions between hydrogen carbonate and the Eu(III) complexes were studied using the Benesi-Hildebrand equation adapted to the values of the asymmetry ratio, as described in the experimental section. Since there is linearity in the plot of $R_0/(R - R_0)$ *vs.* $[HCO_3^-]^{-2}$ for Eu(bpcd)Cl and Eu(bQcd)OTf (Figure 9 and S13) and in the plot of $R_0/(R - R_0)$ *vs.* $[HCO_3^-]^{-1}$ for of Eu(PyC3A) and Eu(QC3A) (Figure 10), the stoichiometry of the hydrogen carbonate adducts is 1:1 for Eu(PyC3A) and Eu(QC3A) complexes and 1:2 for Eu(bpcd)Cl and Eu(bQcd)OTf ones.

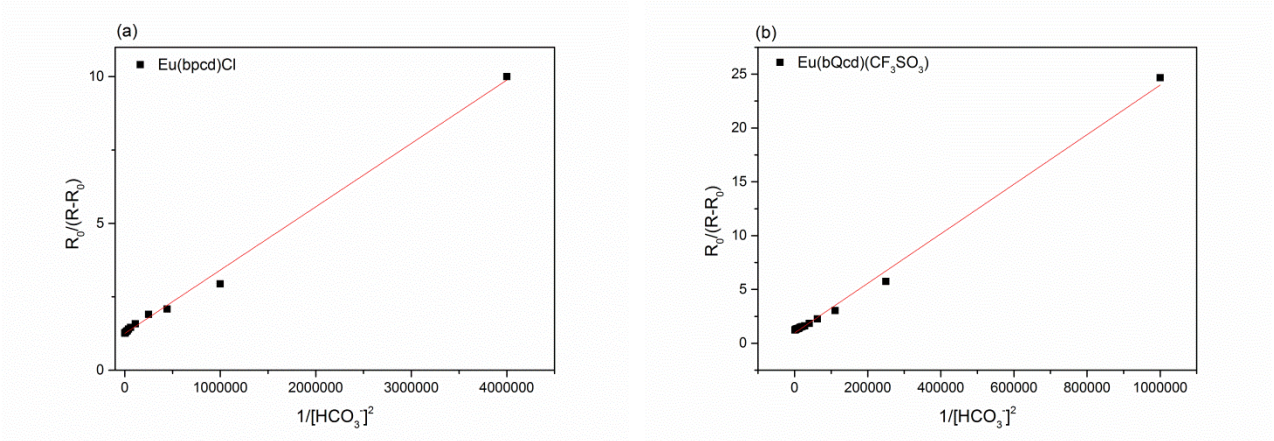


**Figure 9.** Benesi–Hildebrand plot vs $[HCO_3^-]^{2-}$ ($M^{-2}$) for (a) $[Eu(bpcd)]^+$ and (b) $[Eu(bQcd)]^+$ complexes. $R_0$ is the asymmetry ratio of the starting complex; R is the asymmetry ratio after each addition of the analyte. R and $R_0$ have been calculated from the relative Eu(III) luminescence emission spectrum.

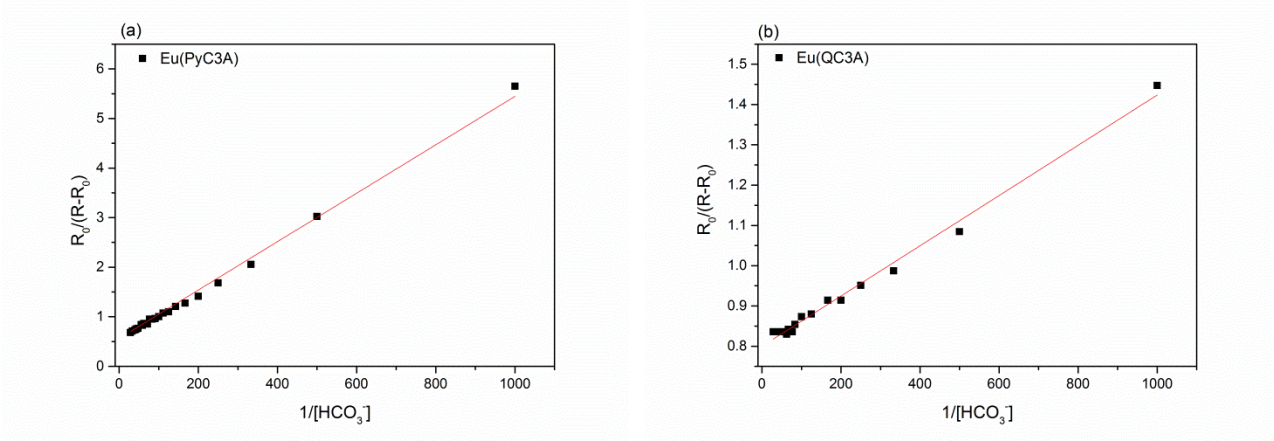


**Figure 10.** Benesi–Hildebrand plot vs $[HCO_3^-]^{-1}$ ($M^{-1}$) for (a) Eu(PyC3A) and (b) Eu(QC3A) complexes. $R_0$ is the asymmetry ratio of the starting complex; R is the asymmetry ratio after each addition of the analyte. R and $R_0$ have been calculated from the relative Eu(III) luminescence emission spectrum.

Since the affinity of the anion for the Ln(III) centre is mainly determined by coulombic attraction it is not surprising that the cationic complexes Eu(bpcd)Cl and Eu(bQcd)OTf can coordinate the hydrogen carbonate anion with high affinity constants (calculated from the ratio of intercept/slope of the Benesi-Hildebrand plot, Table 5). To the best of our knowledge, a value of log*K* higher than 4, in the case of hydrogen carbonate ion, is unprecedented in the literature and this is probably related to the unusual number of target anions bound to the metal center. The Eu(III) in these complexes can bind up to 2 hydrogen carbonate units, likely due, as discussed in the introduction, to the lower number of donating atoms (6-fold coordination) than in the case of ligands commonly employed for Ln(III)-based luminescence anion sensing (NOTA and DOTA-like possessing 7-fold coordination). The possible structures of the 1:2 hydrogen carbonate adducts to $[Y(\textit{trans}\text{-O,O-bpcd})(H_2O)_2]^+$ obtained by DFT calculations (Figure 11) show two possible coordination modes. However, the *bis*-monodentate hydrogen carbonate seems to be the only possible isomer being 10.3 kcal $mol^{-1}$ more stable than the *bis*-bidentate one (also the latter presents an imaginary vibrational mode corresponding to the opening of two Y-O bonds). The optimization of the 1:2 adduct with both hydrogen carbonate coordination modes (one bi- and one mono-dentate) led always to a *bis*-monodentate structure.

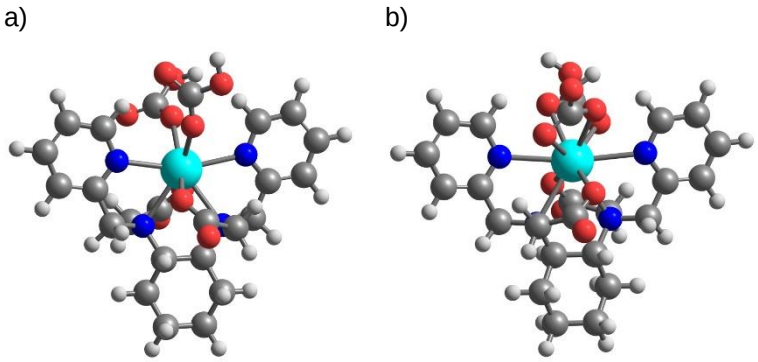


**Figure 11.** Minimum energy structures of the $[Y(\textit{trans}\text{-O,O-bpcd})(HCO_3)_2]^-$ complexes obtained in PCM water with a) *bis*-monodentate and b) *bis*-bidentate hydrogen carbonate coordination modes.

Due to the neutral charge of Eu(PyC3A) and Eu(QC3A) complexes, it is not surprising to find in their adducts with hydrogen carbonate lower binding constants and a 1:1 stoichiometry. It is also reasonable to assume that the negative charge of the 1:1 adduct hampers the formation of the bis-anionic 1:2 species. Furthermore, it is worth to be underlined that the presence of the quinoline ring

affects the stability of the adduct with hydrogen carbonate. In the case of cationic complexes, the adduct with quinoline is less stable than the one with pyridine. On the contrary, an opposite trend is observed for the neutral complexes. The reasons of such behavior in the case of the diacid ligand could be found in the high steric hindrance of the heteroaromatic ring which, at least for the *trans*-O,O-bQcd isomer (Figure 4c), presents two hydrogen atoms pointing towards the inner coordination sphere, thus likely to hinder the coordination of hydrogen carbonate and maybe giving rise to an affinity constant one order of magnitude lower than for the pyridine-based analog. Here, we demonstrate how, thanks to a modulation of the steric hindrance at the metal ion using the different ligands in figure 1, it is possible to tune the affinity (and the selectivity) of the complexes towards $HCO_3^-$.

As far as the affinity of the analogous Tb(III) complexes towards hydrogen carbonate is concerned, we expect a behavior similar to the one observed for Eu(III) derivatives, since Eu(III) and Tb(III) complexes are often isostructural due to the similarity of their ionic radii.[55] As expected, the calculated affinity constant for Tb(bpcd)Cl complex, chosen as representative example, is similar to the one of Eu(bpcd)Cl (Table 5 and Figure S14).

The most efficient and selective optical probes for hydrogen carbonate, capable to detect this anion in *cellulo* or in extracellular fluid, are based on charged and neutral Eu(III) and Tb(III) complexes of heptadentate ligands.[21,65–67] As far as their affinity towards hydrogen carbonate in physiological conditions is concerned, they show a log*K* values in the 2.6 - 3.85 range. The surprising higher affinity of Eu(bQcd)($CF_3SO_3$) and Eu(bpcd)Cl (log*K* 4.62 and 5.76, respectively) promises a better selectivity towards $HCO_3^-$. In this context, since both the enantiomers of the analog Tb(bpcd)Cl weakly interact with L-lactate (log*K* = 1.3 - 1.45),[34] a strong selectivity for hydrogen carbonate is expected in a solution containing both analytes.

**Table 5.** Apparent equilibrium constants (log*K*) constant for the formation of the adducts with hydrogen carbonate ($HCO_3^-$), [complex] + $n$·hydrogen carbonate ⇆ [complex(hydrogen carbonate)$_n$] (T = 298 K, pH 7.40 (±0.05), I = 0.1M NaCl, 40 μM complex), determined through fluorimetric titration. Charges omitted for clarity

| Complex | *n* | log*K* |
|---|---|---|
| Eu(bpcd)Cl/Tb(bpcd)Cl | 2 | 5.76(8)/5.94(8) |
| Eu(bQcd)($CF_3SO_3$) | 2 | 4.62(8) |
| Eu(PyC3A) | 1 | 2.06(8) |
| Eu(QC3A) | 1 | 3.11(8) |

## Conclusions

The cationic **Ln(bpcd)**$^+$ and **Ln(bQcd)**$^+$ complexes and the neutral **Ln(PyC3A)** and **Ln(QC3A)** ones are highly stable in aqueous solution ($9.97 < \log\beta < 15.68$) and they exist as a couple of isomeric compounds differing by the ligand stereochemistry (*trans*-N,N and *trans*-O,O for $bpcd^{2-}$ and $bQcd^{2-}$; *trans*-O,O and *trans*-N,O for $PyC3A^{3-}$ and $QC3A^{3-}$).

For all the complexes, the Ln(III) luminescence intensity increases as a function of the hydrogen carbonate concentration in physiologic solution. The best sensitivity of the optical response towards $HCO_3^-$ in the concentration range related to metabolic acidosis has been observed for **Eu(bpcd)**$^+$ and **Eu(QC3A)** complexes. It has been possible to obtain an unprecedented affinity towards hydrogen carbonate ion by simply playing with several features of the investigated complexes such as: i) the relatively low coordination number of the ligands, which have 6 donating atoms; ii) the positive or neutral charge and iii) the steric hindrance at the metal ion. The positively charged **Eu(bpcd)**$^+$ and **Tb(bpcd)**$^+$ complexes, which possesses a small steric hindrance at the metal ion, reveal the highest logK values (5.76 and 5.94, respectively) reported up to now in the literature, for the formation of an adduct with $HCO_3^-$ characterized by an uncommon 1:2 stoichiometry. With regard to the state-of-art of the optical sensing of hydrogen carbonate ion in extracellular fluid and *in cellulo* experiments, **Ln(bpcd)**$^+$ (Ln = Tb and Eu) can be considered as very promising optical probes with an enhanced selectivity.

**Acknowledgments**

AM acknowledges the University of Udine ("Piano Strategico d'Ateneo") for the grant to acquire the HPC hardware employed in this study.

**References**

1 J. C. G. Bünzli, *Chem.Rev.*, 2010, **110**, 2729–2755.

2 H. Tsukube and S. Shinoda, *Chem. Rev.*, 2002, **102**, 2389–2404.

3 S. J. Butler and D. Parker, *Chem. Soc. Rev.*, 2013, **42**, 1652–1666.

4 J. C. G. Bünzli and S. V. Eliseeva, *Chem. Sci.*, 2013, **4**, 1939–1949.

5 M. C. Heffern, L. M. Matosziuk and T. J. Meade, *Chem. Rev.*, 2014, **114**, 4496–4539.

6 J. W. Walton, A. Bourdolle, S. J. Butler, M. Soulie, M. Delbianco, B. K. McMahon, R. Pal, H. Puschmann, J. M. Zwier, L. Lamarque, O. Maury, C. Andraud and D. Parker, *Chem. Commun.*, 2013, **49**, 1600–1602.

7 D. G. Smith, B. K. McMahon, R. Pal and D. Parker, *Chem. Commun.*, 2012, **48**, 8520–8522.

8 E. A. Weitz, J. Y. Chang, A. H. Rosenfield and V. C. Pierre, *J. Am. Chem. Soc.*, 2012, **134**, 16099–16102.

9 A. Brandner, T. Kitahara, N. Beare, C. Lin, M. T. Berry and P. S. May, *Inorg. Chem.*, 2011, **50**, 6509–6520.

10 J. C. G. Bünzli and S. V. Eliseeva, in *Comprehensive Inorganic Chemistry II (Second Edition): From Elements to Applications*, Elsevier, 2013, vol. 8, pp. 339–398.

11 W. T. Carnall, H. Crosswhite and H. M. Crosswhite, *Energy level structure and transition probabilities in the spectra of the trivalent lanthanides in $LaF_3$*, Argonne, IL (United States), 1978.

12 K. L. Peterson, J. V. Dang, E. A. Weitz, C. Lewandowski and V. C. Pierre, *Inorg. Chem.*, 2014, **53**, 6013–6021.

13 A. G. Weidmann, A. C. Komor and J. K. Barton, *Philos. Trans. R. Soc. A Math. Phys. Eng. Sci.*, 2013, **371**, 20120117.

14 C. A. Puckett and J. K. Barton, *J. Am. Chem. Soc.*, 2007, **129**, 46–47.

15 A. S. Chauvin, F. Thomas, B. Song, C. D. B. Vandevyver and J. C. G. Bünzli, *Philos. Trans. R. Soc. A Math. Phys. Eng. Sci.*, 2013, **371**, 20120295.

16 E. J. New, A. Congreve and D. Parker, *Chem. Sci.*, 2010, **1**, 111–118.

17 B. S. Murray, E. J. New, R. Pal and D. Parker, *Org. Biomol. Chem.*, 2008, **6**, 2085–2094.

18 R. Carr, L. Di Bari, S. Lo Piano, D. Parker, R. D. Peacock and J. M. Sanderson, *Dalton Trans.*, 2012, **41**, 13154.

19 C. P. Montgomery, E. J. New, D. Parker and R. D. Peacock, *Chem. Commun.*, 2008, **0**, 4261.

20 E. A. Weitz and V. C. Pierre, *Chem. Commun.*, 2011, **47**, 541–543.

21 D. G. Smith, R. Pal and D. Parker, *Chem. -Eur. J.*, 2012, **18**, 11604–11613.

22 F. Piccinelli, A. Melchior, A. Speghini, M. Monari, M. Tolazzi and M. Bettinelli, *Polyhedron*, 2013, **57**, 30–38.

23 F. Piccinelli, M. Bettinelli, A. Melchior, C. Grazioli and M. Tolazzi, *Dalton Trans.*, 2015, **44**, 182–192.

24 M. Mihorianu, M. Leonzio, M. Monari, L. Ravotto, P. Ceroni, M. Bettinelli and F. Piccinelli, *ChemistrySelect*, 2016, **1**, 1996–2003.

25 F. Piccinelli, M. Leonzio, M. Bettinelli, M. Monari, C. Grazioli, A. Melchior and M. Tolazzi, *Dalton Trans.*, 2016, **45**, 3310–8.

26 W. N. L. and and N. Sträter, 1996.

27 C. A. Wagner, J. Kovacikova, P. A. Stehberger, C. Winter, C. Benabbas and N. Mohebbi, *Nephron - Physiol.*, 2006, 103, p1-6.

28 J. D. Kopple, K. Kalantar-Zadeh and R. Mehrotra, *Kidney Int. Suppl.*, 2005, **67**, S21–S27.

29 G. Gran, *Analyst*, 1952, **77**, 661.

30 P. Gans, A. Sabatini and A. Vacca, *Talanta*, 1996, **43**, 1739–53.

31 L. Toso, G. Crisponi, V. M. Nurchi, M. Crespo-Alonso, J. I. Lachowicz, D. Mansoori, M. Arca, M. A. Santos, S. M. Marques, L. Gano, J. Niclós-Gutíerrez, J. M. González-Pérez, A. Domínguez-Martín, D. Choquesillo-Lazarte and Z. Szewczuk, *J. Inorg. Biochem.*, 2014, **130**, 112–121.

32 G. H. Jeffrey, J. Bassett, J. Mendham and R. C. Denney, *Vogel's textbook of quantitative chemical analysis*, John Wiley & Sons, 5th edn., 1990, vol. 14.

33 M. Leonzio, A. Melchior, G. Faura, M. Tolazzi, F. Zinna, L. Di Bari and F. Piccinelli, *Inorg. Chem.*, 2017, **56**, 4413–4422.

34 M. Leonzio, A. Melchior, G. Faura, M. Tolazzi, M. Bettinelli, F. Zinna, L. Arrico, L. Di Bari and F. Piccinelli, *New J. Chem.*, 2018, **42**, 7931–7939.

35 P. Di Bernardo, P. L. L. Zanonato, A. Bismondo, A. Melchior and M. Tolazzi, *Dalton Trans.*, 2009, 4236–4244.

36 A. C. Mendonça, A. F. Martins, A. Melchior, S. M. Marques, S. Chaves, S. Villette, S. Petoud, P. L. Zanonato, M. Tolazzi, C. S. Bonnet, É. Tóth, P. Di Bernardo, C. F. G. C. Geraldes and M. A. Santos, *Dalton Trans.*, 2013, **42**, 6046–57.

37 A. D. Becke, *J.Chem.Phys.*, 1993, **98**, 1372–1377.

38 C. T. Lee, W. T. Yang and R. G. Parr, *Phys.Rev.B*, 1988, **37**, 785–789.

39 X. Cao and M. Dolg, *J. Chem. Phys.*, 2001, **115**, 7348–7355.

40 J. Tomasi, B. Mennucci and R. Cammi, *Chem. Rev.*, 2005, **105**, 2999–3093.

41 M. J. Frisch, G. W. Trucks, H. B. Schlegel, G. E. Scuseria, M. A. Robb, J. R. Cheeseman, G. Scalmani, V. Barone, G. A. Petersson, H. Nakatsuji, X. Li, M. Caricato, A. V. Marenich, J. Bloino, B. G. Janesko, R. Gomperts, B. Mennucci, H. P. Hratchian, J. V. Ortiz, A. F. Izmaylov, J. L. Sonnenberg, D. Williams-Young, F. Ding, F. Lipparini, F. Egidi, J. Goings, B. Peng, A. Petrone, T. Henderson, D. Ranasinghe, V. G. Zakrzewski, J. Gao, N. Rega, G. Zheng, W. Liang, M. Hada, M. Ehara, K. Toyota, R. Fukuda, J. Hasegawa, M. Ishida, T. Nakajima, Y. Honda, O. Kitao, H. Nakai, T. Vreven, K. Throssell, J. Montgomery, J. A., J. E. Peralta, F. Ogliaro, M. J. Bearpark, J. J. Heyd, E. N. Brothers, K. N. Kudin, V. N. Staroverov, T. A. Keith, R. Kobayashi, J. Normand, K. Raghavachari, A. P. Rendell, J. C. Burant, S. S. Iyengar, J. Tomasi, M. Cossi, J. M. Millam, M. Klene, C. Adamo, R. Cammi, J. W. Ochterski, R. L. Martin, K. Morokuma, O. Farkas, J. B. Foresman and D. J. Fox, *Gaussian 16 Rev.A03 Wallingford, CT*, 2016.

42 D. F. Eaton, *Pure Appl. Chem.*, 1988, **60**, 1107–1114.

43 H. A. Benesi and J. H. Hildebrand, *J. Am. Chem. Soc.*, 1949, **71**, 2703–2707.

44 P. Polese, M. Tolazzi and A. Melchior, *J. Therm. Anal. Calorim.*, 2018, DOI: 10.1007/s10973-018-7409-2.

45 D. W. Lee, H. J. Ha and W. K. Lee, *Synth. Commun.*, 2007, **37**, 737–742.

46 E. M. Gale, S. Mukherjee, C. Liu, G. S. Loving and P. Caravan, *Inorg. Chem.*, 2014, **53**, 10748–10761.

47 A. V. Rayer, K. Z. Sumon, L. Jaffari and A. Henni, *J. Chem. Eng. Data*, 2014, **59**, 3805–3813.

48 R. Ferreirós-Martínez, D. Esteban-Gómez, C. Platas-Iglesias, A. De Blas and T. Rodríguez-Blas, *Dalt. Trans.*, 2008, 5754–5765.

49 G. Anderegg, *Helv. Chim. Acta*, 1974, **57**, 1340–1346.

50 K. Kahmann, H. Sigel and H. Erlenmeyer, *Helv. Chim. Acta*, 1964, **47**, 1754–1763.

51 H. Kitano, Y. Onishi, A. Kirishima, N. Sato and O. Tochiyama, *Radiochim. Acta*, 2006, **94**, 541–547.

52 P. Caravan, P. Mehrkhodavandi and C. Orvig, *Inorg. Chem.*, 1997, **36**, 1316–1321.

53 M. Wagner, R. Ruloff, E. Hoyer and W. Gründer, *Z. Naturforsch. C.*, 1997, **52**, 508–15.

54 R. M. Smith and A. E. Martell, *Sci. Total Environ.*, 1987, **64**, 125–147.

55 P. Di Bernardo, A. Melchior, M. Tolazzi and P. L. Zanonato, *Coord. Chem. Rev.*, 2012, **256**,

328–351.

56 L. Tei, Z. Baranyai, L. Gaino, A. Forgács, A. Vágner and M. Botta, *Dalt. Trans.*, 2015, **44**, 5467–5478.

57 K. Binnemans, *Coord. Chem. Rev.*, 2015, **295**, 1–45.

58 R. M. Supkowski and W. D. Horrocks, *Inorg. Chim. Acta*, 2002, **340**, 44–48.

59 W. D. Horrocks and D. R. Sudnick, *J. Am. Chem. Soc.*, 1979, **101**, 334–340.

60 W. D. Horrocks, J. P. Bolender, W. D. Smith and R. M. Supkowski, *J. Am. Chem. Soc.*, 1997, **119**, 5972–5973.

61 M. H. V. Werts, R. T. F. Jukes and J. W. Verhoeven, *Phys. Chem. Chem. Phys.*, 2002, **4**, 1542–1548.

62 D. L. Dexter, *J. Chem. Phys.*, 1953, **21**, 836–850.

63 D. Parker, P. K. Senanayake and J. A. G. Williams, *J. Chem. Soc. Perkin Trans. 2*, 1998, **0**, 2129–2140.

64 C. Li, Y. Liu, Y. Wu, Y. Sun and F. Li, *Biomaterials*, 2013, **34**, 1223–1234.

65 Y. Bretonniere, M. J. Cann, D. Parker and R. Slater, *Org. Biomol. Chem.*, 2004, **2**, 1624–1632.

66 S. J. Butler, B. K. McMahon, R. Pal, D. Parker and J. W. Walton, *Chem. - A Eur. J.*, 2013, **19**, 9511–9517.

67 D. Imperio, G. B. Giovenzana, G. L. Law, D. Parker and J. W. Walton, *Dalt. Trans.*, 2010, **39**, 9897–9903.